Khadak Singh Mahata | Maheswar Rupakheti | Arnico Kumar Panday | Piyush Bhardwaj | Manish Naja | Ashish Singh | Andrea Mues | Paolo Cristofanelli | Deepak Pudasainee | Paolo Bonasoni | Mark G. Lawrence

Observation and analysis of spatio-temporal characteristics of surface ozone and carbon monoxide at multiple sites in the Kathmandu Valley, Nepal

Suggested citation referring to the original publication:
Atmospheric Chemistry and Physics Discussions (2017)
DOI https://doi.org/10.5194/acp-2017-709
ISSN (print) 1680-7367
ISSN (online) 1680-7375

Atmos. Chem. Phys. Discuss., https://doi.org/10.5194/acp-2017-709
Manuscript under review for journal Atmos. Chem. Phys.
Discussion started: 18 December 2017

Atmospheric Chemistry and Physics Discussions

Observation and analysis of spatio-temporal characteristics of surface ozone and carbon monoxide at multiple sites in the Kathmandu Valley, Nepal

Khadak Singh Mahata[1,2], Maheswar Rupakheti[1,3], Arnico Kumar Panday [4,5], Piyush Bhardwaj[6], Manish Naja[6], Ashish Singh[1], Andrea Mues[1], Paolo Cristofanelli[7], Deepak Pudasainee[8], Paolo Bonasoni[7], Mark G. Lawrence[1,2]

[1]Institute for Advanced Sustainability Studies (IASS), Potsdam, Germany

[2]University of Potsdam, Potsdam, Germany

[3]Himalayan Sustainability Institute (HIMSI), Kathmandu, Nepal

[4]International Centre for Integrated Mountain Development (ICIMOD), Lalitpur, Nepal

[5]University of Virginia, Charlottesville, USA

[6]Aryabhatta Research Institute of Observational Sciences (ARIES), Nainital, India

[7]CNR-ISAC, National Research Council of Italy – Institute of Atmospheric Sciences and Climate, Bologna, Italy

[8]Department of Chemical and Materials Engineering, University of Alberta, Edmonton, Canada

Correspondence to: Maheswar Rupakheti (maheswar.rupakheti@iass-potsdam.de) and Khadak Singh Mahata (khadak.mahata@iass-potsdam.de)

Atmos. Chem. Phys. Discuss., https://doi.org/10.5194/acp-2017-709
Manuscript under review for journal Atmos. Chem. Phys.
Discussion started: 18 December 2017

Atmospheric Chemistry and Physics Discussions

Abstract

Residents of the Kathmandu Valley experience severe particulate and gaseous air pollution throughout most of the year, even during much of the rainy season. The knowledge base for understanding the air pollution in the Kathmandu Valley was previously very limited, but is improving rapidly due to several field measurement studies conducted in the last few years. Thus far, most analyses of observations in the Kathmandu Valley have been limited to short periods of time at single locations. This study extends on the past studies by examining the spatial and temporal characteristics of two important gaseous air pollutant (CO and O_3) based on simultaneous observations over a longer period at five locations within the valley and on its rim, including a supersite (at Bode in the valley center, 1345 m above sea level) and four satellite sites (at Paknajol, 1380 m asl in the Kathmandu city center, at Bhimdhunga (1522 m asl), a mountain pass on the valley's western rim, at Nagarkot (1901 m asl), another mountain pass on the eastern rim, and Naikhandi, near the valley's only river outlet). CO and O_3 mixing ratios were monitored from January to July 2013, along with other gases and aerosol particles by instruments deployed at the Bode supersite during the international air pollution measurement campaign SusKat-ABC (Sustainable Atmosphere for the Kathmandu Valley – endorsed by the Atmospheric Brown Clouds program of UNEP). The O_3 monitoring at Bode, Paknajol and Nagarkot as well as the CO monitoring at Bode were extended beyond July 2013 to investigate their variability over a complete annual cycle. Higher CO mixing ratios were found at Bode than at the outskirt sites (Bhimdhunga, Naikhandi and Nagarkot), and all sites except Nagarkot showed distinct diurnal cycles of CO mixing ratio with morning peaks and daytime lows. Seasonally, CO was higher during the pre-monsoon and winter seasons, especially due to the emissions from brick kiln industries, which only operate during this period, as well as increased domestic heating during winter, and regional forest fires and agro-residue burning. It was lower during the monsoon due to rainfall, which reduces open burning activities within the valley and in the surrounding regions, and thus reduces the sources of CO. The meteorology of the valley also played a key role in determining the CO mixing ratios. Furthermore, there was evidence of some influence of pollution from the greater region around the valley. A top-down estimate of the CO emission flux was made by using the CO mixing ratio and mixing layer height (MLH) measured at Bode. The estimated annual CO flux at Bode was 4.92 μg m^{-2} s^{-1}, which is 2-14

Atmos. Chem. Phys. Discuss., https://doi.org/10.5194/acp-2017-709
Manuscript under review for journal Atmos. Chem. Phys.
Discussion started: 18 December 2017

Atmospheric Chemistry and Physics Discussions

55 times higher than that in widely used emission inventory databases (EDGAR HTAP, REAS and
56 INTEX-B). This difference in CO flux between Bode and other emission databases likely arises
57 from large uncertainties in both the top-down and bottom-up approaches to estimating the
58 emission flux. The O_3 mixing ratio was found to be highest during the pre-monsoon season at all
59 sites, while the timing of the seasonal minimum varied across the sites. The daily maximum 8
60 hour average O_3 exceeded the WHO recommended guideline of 50 ppb on more days at the
61 hilltop station of Nagarkot (159/357 days) than at the urban valley bottom sites of Paknajol
62 (132/354 days) and Bode (102/353 days), presumably due to the influence of free-tropospheric
63 air at the high-altitude site, as well as to titration of O_3 by fresh NOx emissions near the urban
64 sites. More than 78% of the exceedance days were during the pre-monsoon period at all sites.
65 This was due to both favorable meteorological conditions as well as contributions of precursors
66 from regional sources such as forest fires and agro-residue burning. The high O_3 mixing ratio
67 observed during the pre-monsoon period is of a high concern for human health and ecosystems,
68 including agroecosystems in the Kathmandu Valley and surrounding regions.

69

70 1. Introduction

71 Air pollution is one of the major health risks globally. It was responsible for premature loss of
72 about 7 million lives worldwide in 2012 (WHO, 2014), with about 1.7 million of these being in
73 South Asian countries (India, Pakistan, Nepal and Bangladesh) in 2013 (Forouzanfar, 2015).
74 South Asia is considered to be a major air pollution hotspot (Monks et al., 2009) and it is
75 expected to be one of the most polluted regions in the world for surface ozone (O_3) and other
76 pollutants by 2030 (Dentener et al., 2006; IEA 2016; OECD 2016). Past studies have shown that
77 the air pollution from this region affects not only the region itself, but is also transported to other
78 parts of the world, including comparatively pristine regions such as the Himalayas and the
79 Tibetan plateau (Bonasoni et al., 2010; Ming, et al., 2010; Lüthi et al., 2015), as well as to other
80 distant locations such as northern Africa and the Mediterranean (Lawrence and Lelieveld, 2010).
81 The air pollution problem is particularly alarming in many urban areas of South Asia, including
82 in the city of Kathmandu and the broader Kathmandu Valley, Nepal (Chen et al., 2015; Putero et
83 al., 2015; Kim et al., 2015; Sarkar et al., 2016; Shakya et al., 2017). This is due to their rapid
84 urbanization, economic growth and the use of poor technologies in the transportation, energy and

industrial sectors. Effectively mitigating air pollutants in the regions like the Kathmandu Valley requires scientific knowledge about characteristics and sources of the pollutants. To contribute to this urgently-needed scientific knowledge base, in this study we focus on the analysis of measurements of two important gaseous species, carbon monoxide (CO), an urban air pollution tracer, and O_3, at multiple sites in and around the Kathmandu Valley. This study analyzes data from January 2013 to March 2014, which includes the intensive phase of an international air pollution measurement campaign – SusKat-ABC (Sustainable Atmosphere for the Kathmandu Valley – Atmospheric Brown Clouds) – conducted during December 2012 - June 2013 (Rupakheti et al., 2017, manuscript in preparation, submission anticipated in 1-2 months), with measurements of O_3 and CO at some sites continuing beyond the intensive campaign period (Bhardwaj et al., 2017; Mahata et al., 2017).

CO is a useful tracer of urban air pollution as it is primarily released during incomplete combustion processes. It is also toxic at high concentrations indoors, but our focus here is on ambient levels. The main anthropogenic sources of CO in the Kathmandu Valley are vehicles, cooking activities (using liquefied petroleum gas, kerosene, and firewood), and industries, including brick kilns, especially biomass co-fired kilns with older technologies, and until recently diesel power generator sets (Panday and Prinn, 2009; Kim et al, 2015; Sarkar et al., 2016; Mahata et al., 2017; Sarkar et al., 2017). Tropospheric ozone, which is formed by photochemical reactions involving oxides of nitrogen (NO_x) and volatile organic compounds (VOCs), is a strong oxidizing agent in the troposphere. Because of its oxidizing nature, it is also deleterious to human health and plants already at typically polluted ambient levels (Lim et al., 2012; Burney and Ramanathan, 2014; Feng, 2015; Monks et al., 2015). Tropospheric O_3 is estimated to be responsible for about 5-20 % of deaths caused by air pollution globally (Brauer et al., 2012; Lim et al., 2012; Silva et al., 2013). It has also been estimated that high concentrations of O_3 are responsible for a global loss of crops equivalent to $ 11-18 billion annually (Avnery et al., 2011; UNEP and WMO, 2011), a substantial fraction of which is associated with the loss in wheat in India alone (equivalent to $ 5 billion in 2010) (Burney and Ramanathan, 2014). O_3 can also serve as a good indicator of the timing of the breakup of the nighttime stable boundary layer (when the ozone levels increase rapidly in the morning due to downward transport from the free troposphere (Panday and Prinn, 2009; Geiß et al., 2017)

Only a few past studies have measured ambient CO mixing ratios in the Kathmandu Valley. Davidson et al. (1986) measured CO in the city center and found mixing ratios between 1 and 2.5 ppm in the winter of 1982-1983. Panday and Prinn (2009) measured similar levels of CO mixing ratios during September 2004 – June 2005, although the main sources of CO shifted from biofuel-dominated air pollutants from cooking activities in the 1980s to vehicle-dominated pollutants in the 2000s. The growth rate in the vehicle fleet has had a substantial influence on air pollution in the valley, including CO and O_3. Out of 2.33 million vehicles in Nepal, ~50% of them are in the Kathmandu Valley (DoTM, 2015). Shrestha et al. (2013) estimated 31 kt of annual emission of CO from a fraction of the vehicle fleet in the Kathmandu Valley in 2010 by using data from a field survey as input data to the International Vehicle Emission (IVE) model. The model simulation considered motorcycles, buses, taxis, vans and three wheelers, but did not include personal cars, trucks and non-road vehicles. The studied fleets covered ~73% of the total fleet (570 145) registered in the valley in 2010, with motorcycles being the most common vehicle (69%) within the total fleet.

Past studies have investigated the diurnal and seasonal variations of CO and O_3 mixing ratios in the Kathmandu Valley. Panday and Prinn (2009) observed distinct diurnal variations of CO mixing ratios and particulate matter concentrations observed during September 2004 – June 2005 at Bouddha (about 4 km northwest of the SusKat-ABC supersite at Bode), with morning and evening peaks. It was found in the Kathmandu Valley that such peaks were created by the interplay between the ventilation, as determined by the local meteorology, and the timing of emissions, especially traffic and cooking emissions. The morning CO peak was also associated with the recirculation of the pollutants transported down from an elevated residual pollution layer (Panday and Prinn, 2009).

O_3 was observed to have lower nighttime levels in the city center than at the nearby hilltop site of Nagarkot (Panday and Prinn, 2009). Pudasainee et al. (2006) studied the seasonal variations of O_3 mixing ratios based on the observation for a whole year (2003-2004) in Pulchowk in the Lalitpur district, just south of central Kathmandu Metropolitan City (KMC) in the Kathmandu Valley. They reported seasonal O_3 mixing ratios to be highest during the pre-monsoon and lowest in the winter. As a part of the SusKat-ABC Campaign, Putero et al. (2015) monitored O_3 mixing ratios at Paknajol, an urban site in the center of the KMC over a full-year period

(February 2013-January 2014). They also observed similar seasonal variations in O_3 mixing ratios in the valley to those observed by Pudasainee et al. (2006), with highest O_3 during the pre-monsoon season, followed by the monsoon, post-monsoon and winter seasons. They found that during the pre-monsoon season, westerly winds and regional synoptic circulation transport O_3 and its precursors from regional forest fires located outside the Kathmandu Valley. In another study conducted as part of the SusKat-ABC Campaign, 37 non-methane volatile organic compounds (NMVOCs) were measured at Bode, with data recording every second, during winter of 2012-2013; the measurements included isoprene, an important biogenic precursor of O_3 (Sarkar et al., 2016). They found concentrations to vary in two distinct periods. The first period was marked by no brick kiln operations and was associated with high biogenic emissions of isoprene. During the second period nearby brick kilns, which use coal mixed with biomass, were in operation that contributed to elevated concentrations of ambient acetonitrile, benzene and isocyanic acid. Furthermore, they found that oxygenated NMVOCs and isoprene combined accounted for 72% and 68% of the total O_3 production potential in the first period and second period, respectively.

Prior to the SusKat-ABC campaign there were no studies that simultaneously measured ambient CO and O_3 mixing ratios at multiple sites in the Kathmandu Valley over extended periods of time. Past studies either focused on one long-term site, or on short-term observation records at various sites (Panday and Prinn, 2009), or they investigated the seasonal characteristics of single pollutants such as O_3 at a single site in the valley (Pudasainee et al., 2006). The most comparable past study is by Putero et al. (2015), who described O_3 mixing ratios at one SusKat-ABC site (Paknajol) in the Kathmandu city center observed during the SusKat-ABC campaign, and discussed O_3 seasonal variations. There is also a companion study on regional CO and O3 pollution by Bhardwaj et al. (2017) which is based on O_3 and CO mixing ratios monitored at the SusKat-ABC supersite at Bode in the Kathmandu Valley for a limited period (January-June 2013) and at two sites in India (Pantnagar in Indo-Gangetic Plain and Nainital in Himalayan foothill). They reported simultaneous enhancement in O_3 and CO levels at these three sites in spring, highlighting contribution of regional emissions, such as biomass burning in northwest Indo-Gangetic Plain (IGP), and regional transport to broader regional scale pollution, including in the Kathmandu Valley. In this study, we document the diurnal and seasonal (where applicable) characteristics and spatial distributions of CO and O_3 mixing ratios based on simultaneous

observations at several locations within the valley and on the valley rim mountains over a full year, helping to characterize the pollution within the valley and the pollution plume entering and exiting the valley. We also compute the first top-down estimates of CO emission fluxes for the Kathmandu Valley and compare these to CO emissions fluxes in widely-used emission datasets such as EDGAR HTAP (Janssens-Maenhout et al., 2000), REAS (Kurokawa et al., 2013) and INTEX-B (Zhang et al., 2009).

2. Study sites and methods

The Kathmandu Valley, situated in the foothills of the Central Himalaya, is home to more than 3 million people. The valley floor has an area of about 340 km^2, with an average altitude of about 1300 m above sea level (m asl). It is surrounded by peaks of about 1900-2800 m asl. The valley has five major mountain passes on its rim: the Nagdhunga, Bhimdhunga and Mudku Bhanjhyang passes in the west, and the Nala and Nagarkot passes in the east as shown in Figure 1. The passes are situated at altitudes of 1480-1530 m asl. There is also one river outlet (the Bagmati River) towards the southwest, which constitutes a sixth pass for air circulation in and out of the valley (Regmi et al., 2003; Panday and Prinn, 2009). We selected five measurement sites, including two on the valley floor (Bode and Paknajol), two on mountain ridges (Bhimdhunga and Nagarkot) and one near the Bagmati River outlet (Naikhandi) to characterize the spatial and temporal variabilities of CO and O_3 mixing ratios in the Kathmandu Valley. A short description of the measurement sites is presented here and in Table 1, and details on instruments deployed at those sites for this study are presented in Table 2. Further details of the measurement sites are described in the SusKat-ABC campaign overview paper (Rupakheti et al., 2017, manuscript in preparation).

Bode: This was the supersite of the SusKat-ABC Campaign. Bode (27.69°N and 85.40°E, 1344 m asl) is located in the Madhyapur Thimi municipality in the eastern part of the valley. It is a semi-urban site surrounded by scattered urban buildings and residential houses in agricultural lands. There are 10 brick kilns and the Bhaktapur Industrial Estate towards the southeast direction, within 4 km distance from the site (refer to Sarkar et al., 2016; Mahata et al., 2017 for details). The O_3 and CO instruments at Bode site were placed on the fifth floor of a 6-story building, the tallest in the area.

Bhimdhunga: This site (27.73°N, 85.23°E, 1522 m asl) is located on the Bhimdhunga pass on the western rim of the valley. It sits on the mountain ridge between the Kathmandu Valley to the east and a valley of a tributary of the Trishuli River to the west. It is situated about 5.5 km from the western edge (Sitapaila) of the KMC in a rural setting with only a few scattered rural houses nearby. The CO instrument was placed on the ground floor of a small one-story building and an automatic weather station, AWS (Hobo Onset, USA) was set up on the roof of another one-story building at a distance of ca. 15 m from the first building.

Paknajol: This site (27.72°N, 85.30°E, 1380 m asl) is located at the city center in the KMC, near the most popular touristic area (Thamel). It is in the western part of the valley and about 10 km distance from the Bode supersite. The O_3 and metrological instruments relevant to this study were placed on the top floor and rooftop of a 6-story building, the tallest in the area (detail in Putero et al., 2015; note that CO was not measured here).

Naikhandi: This site (27.60°N, 85.29°E, 1233 m asl) is located within the premises of a school (Kamdhenu Madhyamik Vidhyalaya) located at the southwestern part of the valley (~7 km south from the nearest point of the Ring Road). The school premise is open, surrounded by sparsely scattered rural houses in agricultural lands. The nearest village (~75 houses) is about 500 m away in the southwest direction. There are 5 brick kilns within 2 km distance (2 to the north and 3 to the northeast) from the site. The instruments were kept in a one-story building of the school. The AWS (Hobo Onset, USA) was installed on the ground near the Bagmati River, ~100 m away from the main measurement site.

Nagarkot: This site is located on a mountain ridge (27.72°N, 85.52°E, 1901 m asl), ca. 13 km away to the east from Bode, in the eastern part of the valley. The site faces the Kathmandu Valley to the west and small rural town, Nagarkot, to the east. The instruments were set up in a 2-story building of the Nagarkot Health Post and the AWS (Vaisala WXT520, Finland) was set up on the roof of the building.

Bhimdhunga in the west and Naikhandi near the Bagmati River outlet in the southwest are the most important pass and river outlet for the valley. The Bhimdhunga and Naikhandi sites are

238 approximately 5.5 and 7 km away from the nearest edge of the major city, respectively.
239 Similarly, Bode is located downwind of the city centers and thus receives pollution outflow from
240 nearby city centers such as Kathmandu and Lalitpur due to strong westerly and southwesterly
241 winds (4-6 m s^{-1}) during the day time, and emissions from the Bhaktapur area to the east and
242 southeast direction by calm easterly winds (< 1 m s^{-1}) during the night (Sarkar et al., 2016;
243 Mahata et al., 2017).
244
245 A freshly calibrated new CO analyzer (Horiba APMA-370, Japan) was deployed for the first
246 time at Bode. It is based on the IR absorption method at 4.6 µm by CO molecules. Before field
247 deployment at Bode, it was compared with the bench model of the Horiba (APMA-370), and the
248 correlation (r) between them was 0.9 and slope was 1.09. The instrument was regularly
249 maintained by running auto-zero checks (Bhardwaj et al., 2017). Similarly, another CO analyzer
250 (Picarro G2401, USA) which is based on cavity ring-down spectroscopy technique (CRDS) was
251 also a new factory calibrated unit, and was deployed in Bode along with the Horiba APMA-370.
252 The three-month inter-comparison between the Horiba and Picarro CO measurements had a
253 correlation coefficient of 0.99 and the slope was 0.96 (Mahata et al., 2017). All other CO
254 analyzers (Thermo Scientific, 48i, USA), which are also based on IR absorption by CO
255 molecules, deployed at Bhimdhunga, Naikhandi and Nagarkot, were set up for regular automatic
256 zero checks on a daily basis. In addition, a span check was also performed during the
257 observations by using span gas of 1.99 ppm (Gts-Welco, PA, USA) on March 8, 2013 at
258 Naikhandi and Nagarkot, and on March 9 at Bhimdhunga.
259
260 For the O_3 monitor (Teledyne 400E, USA) at Bode, the regular zero and span checks were
261 carried out using the built-in O_3 generator and scrubber (Bhardwaj et al., 2017). This unit was
262 used in Bode from 01 January 2013 to 09 June 2013. New factory-calibrated O_3 monitors
263 (Thermo Scientific, 49i, USA) were used for the rest of the measurement period (18 June 2013 to
264 31 December 2013) at Bode, and for the full year of measurements at Nagarkot. A Thermo
265 Environmental O_3 analyzer (Model 49i, USA) was used at the Paknajol site (Putero et al., 2015)
266 with the same experimental set up as described in Cristofanelli et al. (2010). The working
267 principle of all of the O_3 instruments is based on the attenuation of UV radiation by O_3 molecules
268 at ~254 nm.

Atmos. Chem. Phys. Discuss., https://doi.org/10.5194/acp-2017-709
Manuscript under review for journal Atmos. Chem. Phys.
Discussion started: 18 December 2017

In order to characterize the observations across the seasons, we considered the following seasons as defined in Shrestha et al. (1999) and used in other previous studies in the Kathmandu Valley (Sharma et al., 2012; Chen et al., 2016; Mahata et al, 2017): Pre-monsoon (March, April, May); Monsoon (June, July, August September); Post-monsoon (October, November); and Winter (December, January, February).

3. Results and discussion

3.1 CO mixing ratio at multiple sites

Figure 2 shows the time series of the hourly average CO mixing ratios at the four sites (Bode, Bhimdhunga, Naikhandi and Nagarkot). Fluctuations in CO mixing ratios were higher during the winter and pre-monsoon than during the monsoon season at all sites. The monsoon rain generally starts in Nepal around mid-June. In 2013, however, there were more frequent rain events in the month of May than in previous years. The CO mixing ratios (measured in parts per billion by volume, hereafter the unit is denoted as ppb) averaged over the total observation periods at four sites were: Bode (569.9 ± 383.5) ppb during 1 January - 15 July, Bhimdhunga (321.5 ± 166.2) ppb during 14 Jan - 15 July, Naikhandi (345.4 ± 147.9) ppb during 3 January - 6 June and Nagarkot (235.5 ± 106.2) ppb during 13 February - 15 July (except 4 April to 7 June). Nagarkot had only about 3 months of CO data (due to problem in zero tests of the instrument) during the observation period. For the measurement period, the CO mixing ratio at Nagarkot (~13 km far from Bode) showed small fluctuations compared with the other sites. High CO values in the Kathmandu Valley during the dry season (November-May) were also reported by Panday and Prinn (2009) based on their measurements during September 2004-May 2005 at Bouddha (~ 4 km in northwest from Bode). The simultaneous episodes of high CO observed in April (1-15) in Bhimdhunga, Bode and Naikhandi indicate the influence of regional sources, in addition to local sources. This is discussed further in section 3.2.3.

3.2 Diurnal and seasonal variations of CO

3.2.1 Diurnal pattern of CO at multiple sites

Figure 3 shows the diurnal cycles of CO mixing ratios at four sites (plotted for the period of 13 February to 3 April 2013, when the data were available from all four sites). The variation in the

299 mixing ratios during the day was characterized by a pronounced morning peak, a weaker evening
300 peak, and a daytime low; except at Nagarkot where peaks are less visible. Multiple sources
301 contribute to the morning and evening peaks, especially emission from vehicles, residential
302 burning (fossil fuel and biomass), brick kilns and trash burning (Kim et al., 2015; Sarkar et al.,
303 2016; Mahata et al., 2017). The observed diurnal cycle of CO is similar to that reported in a
304 previous study (Panday and Prinn, 2009), and is also similar to the diurnal pattern of black
305 carbon (BC) in the Kathmandu Valley (Sharma et al., 2012; Mues et al., 2017). The diurnal
306 cycles of these primary pollutants are closely coupled with the valley's boundary layer height,
307 which is about 1200 m during daytime, and falls to approximately 200 m at nighttime in Bode
308 (Mues et al., 2017). Nagarkot and Bhimdhunga, both on mountain ridges, are generally above the
309 valley's boundary layer, especially at night, and thus the diurnal profile especially at Nagarkot is
310 distinct compared to other three sites, being relatively flat with small dip during 12:00-18:00.
311
312 Clear morning peaks were observed in Bode, Bhimdhunga and Naikhandi at 08:00, 09:00, and
313 10:00, respectively, i.e., the morning peak lags by 1-2 hours in Bhimdhunga and Naikhandi
314 compared to Bode. Bhimdhunga on the mountain ridge may receive the Kathmandu Valley's
315 pollution due to upslope winds (~2 m s^{-1}) from the southeast direction in the morning hours after
316 the dissolution of the valley's boundary layer due to radiative heating of the mountain slopes. On
317 the other hand, Naikhandi is in close proximity to brick kilns and could be impacted by their
318 plumes carried to the site by northerly winds in the early morning (ca. 07:00-10:00, not shown).
319 The evening peak values at Bode and Bhimdhunga were less pronounced compared to their
320 morning maxima. The morning peak at Bode was influenced by nighttime accumulation of CO
321 from nearby brick kilns. Similarly, the local pollution from the nearby village and city area due
322 to upslope winds from the valley floor is expected to contribute to the morning peak at
323 Bhimdhunga. The evening peak at Naikhandi was at 21:00 and was closer to the morning values
324 in comparison to the large difference between morning and evening peaks at Bode and
325 Bhimdhunga. A nighttime build-up of various pollutants compared to the afternoon minimum
326 was typically observed in Bode during the SusKat-ABC measurement period, including the main
327 campaign period (Sarkar et al., 2016; Mahata et al., 2017; Mues et al., 2017). This is mainly
328 associated with the nocturnal decrease in height of the planetary boundary layer, along with
329 persistent emissions such as those from brick kilns, which are in close proximity to the Bode

measurement site. There appears to be less influence of nighttime polluting sources at Naikhandi and Bhimdhunga than at Bode.

The low daytime CO mixing ratios observed at all sites were partly due to the evolution of mixing layer and the entrainment of cleaner air from above the boundary layer after the dissolution of nocturnal stable boundary layer. High wind speeds (4-6 m s^{-1}) during daytime also support turbulent vertical diffusion, as well as flushing of the pollution by less polluted air masses from outside the valley, with stronger horizontal winds allowing significant transport of air masses into the valley. In addition, reduced traffic and household cooking activities during daytime compared to morning and evening rush hours contribute to the reduced mixing ratios.

3.2.2 CO diurnal variation across seasons

Due to the lack of availability of simultaneous CO data at all sites covering the entire sampling period, a one-month period was selected for each season to examine the diurnal variation across the seasons, and to get more insights into the mixing ratios at different times of the day, as reported in Table 4. Figure 4 shows the diurnal variation of CO mixing ratios in Bode, Bhimdhunga, and Naikhandi during the selected periods for the three seasons.

The diurnal cycles during each season had different characteristics. The most prominent distinction was that the CO mixing ratio was low during the monsoon period over all sites (Figure 4, Table 4) as a result of summer monsoon rainfall in the valley, which is 60 - 90% of the 1400 mm rainfall for a typical year (Nayava, 1980; Giri et al., 2006). The rainfall diminishes many burning activities (forest fires, agro-residue and trash burning, and the brick kilns) within the valley and surrounding region, and thus reduces CO emissions. Afternoon CO mixing ratios were higher in the pre-monsoon season than in the other two seasons in Bode, Bhimdhunga and Naikhandi (also see Table 4), with the most likely sources being emissions from forest fires and agro-residue burning arriving from outside the valley during this season (this will be discussed further in section 3.2.3). Nighttime accumulation was observed in Bode and Bhimdhunga, but not at Naikhandi, where the mixing ratio decreased slightly from about 20:00 until about 04:00, after which the mixing ratios increased until the morning peak. The nighttime accumulation of CO in Bode during pre-monsoon and winter is apparently due to the influence of nearby brick

kilns (Mahata et al., 2017). Bhimdhunga is not near any major polluting sources such as brick kilns, and it is unclear whether the nighttime CO accumulation in Bhimdhunga is primarily due to ongoing local residential pollution emissions, and/or to pollution transported from remote sources. The transition of the wind from westerlies during the day to easterlies during the night, with moderate wind speed (~2-4 m s^{-1}) at Bhimdhunga, may bring polluted air masses westwards which were initially transported to the eastern part from the Kathmandu Valley during the daytime (Regmi et al., 2003; Panday and Prinn, 2009; Panday et al., 2009).

Across the seasons, the afternoon (12:00-16:00) CO mixing ratio was higher during the pre-monsoon than in the winter at all three stations (p value for all sites < 0.5) (Table 4), although the mixing layer was higher in the pre–monsoon season than in the winter in Bode (and presumably at the other sites as well). This is not likely to be explained by local emissions in the valley, since these are similar in the winter and pre-monsoon periods. Putero et al. (2015) suggested instead that this reflects an influx of polluted air into the valley due to large synoptic circulation patterns during the pre-monsoon season. Such regional influences are explored further in the next section.

3.2.3 Regional influence on CO in the valley

Recent studies have indicated the likelihood of regional long-range transport contributing to air pollution in different parts of Nepal (Marinoni et al., 2013; Tripathee et al., 2014; Dhungel et al., 2016; Rupakheti et al., 2016; Lüthi et al., 2016; Wan et al., 2017), including the Kathmandu Valley, especially during the pre-monsoon period (Panday and Prinn, 2009; Putero et al., 2015; Bhardwaj et al., 2017). During the pre-monsoon season, frequent agro-residue burning and forest fires are reported in the IGP region including southern Nepal and the Himalayan foothills in India and Nepal (Ram and Sarin, 2010; Vadrevu et al., 2012), and in the Kathmandu Valley. This season is also characterized by the strongest daytime local wind speeds (averaging 4-6 m s^{-1}) in the Kathmandu Valley (Mahata et al., 2017). Our study also observed several episodes of days with both elevated CO mixing ratios (Figure 2) and O_3 mixing ratios (also measured in parts per billion by volume, hereafter the unit is denoted as ppb) (Figure 5) during April and May, especially during the late afternoon period. The influence of regional pollutants was investigated by comparing a 2-week period with normal CO levels (16–30 March (hereafter “period I”) with

391 an adjacent two week period (1-15 April) with episodically high CO mixing ratios (hereafter
392 "period II"), which nicely fit with the "burst" in regional fire activity presented by Putero et al.
393 (2015) in their Figure 9. The t-test of the two data means in period I and period II at Bode,
394 Bhimdhunga and Naikhandi were performed at 95% confidence level and the differences were
395 found to be statistically significant ($p < 0.5$).

396 Figure 5a shows the diurnal cycle of CO mixing ratios during period I (faint color) and period II
397 (dark color) at Bode, Bhimdhunga and Naikhandi. The difference between two periods was
398 calculated by subtracting the average of period I from average of period II. The average CO
399 mixing ratios during period II were elevated with respect to period I by 157 ppb at Bode, 175
400 ppb at Bhimdhunga, and 176 ppb at Naikhandi. The enhancements in mixing ratios at three sites
401 were fairly similar from hour to hour throughout the day, with the exception of the late afternoon
402 when the enhancement was generally greatest. This consistency across the sites suggests that the
403 episode was caused by a large-scale enhancement (regional contribution) being added onto the
404 prevailing local pollution levels at all the sites. A large-scale source would also be consistent
405 with the greater enhancements of CO at the outskirt sites, which would be most directly affected
406 by regional pollution, compared to the central valley site of Bode with strong local sources. The
407 enhancement during the period II is substantial (statistically significant as mentioned above),
408 representing an increase of approximately 45% at the outskirt sites of Bhimdhunga and
409 Naikhandi (which start with lower CO levels), and 23% at Bode. During both periods I and II,
410 local winds from west (the opposite direction from the brick kilns, which were mostly located to
411 the southeast of Bode) were dominant during daytime at Bode (Figure 5b, c). This suggests that
412 the elevation in CO levels was caused by additional emissions in period II in the regions to the
413 west and southwest of the Kathmandu Valley, e.g., large scale agricultural burning and forest
414 fires during this period, as also noted by Putero et al. (2015) (see their Figure 9). Far away, in
415 Lumbini in the southern part of Nepal (Rupakheti et al., 2016), and Pantnagar in northern IGP in
416 India (Bharwdwaj et al., 2017), about 220 km (aerial distance) to the southwest and 585 km to
417 the west, respectively, of the Kathmandu Valley, CO episodes were also observed during the
418 spring season of 2013, providing a strong indication that the episode in period II was indeed
419 regional in nature.

420

Atmos. Chem. Phys. Discuss., https://doi.org/10.5194/acp-2017-709
Manuscript under review for journal Atmos. Chem. Phys.
Discussion started: 18 December 2017

421 **3.3 O_3 in the Kathmandu Valley and surrounding areas**

422 Figure 6 shows the hourly average and daily maximum 8-hour average of O_3 mixing ratios at
423 Bode, Paknajol, and Nagarkot from measurements during the SusKat campaign and afterwards,
424 along with O_3 mixing ratios from a previous study (November 2003 - October 2004; Pudasainee
425 et al., 2006) at the Pulchowk site (4 km away from Paknajol) in the Latitpur district. The daily
426 maximum 8-hour average O_3 was calculated by selecting the maximum O_3 mixing ratio from 8
427 hour running averages during each day. The nighttime mixing ratio of hourly O_3 drops close to
428 zero in Bode, Paknajol and Pulchowk in the winter season. This is a typical characteristic of
429 many urban areas where reaction with NO at night depletes O_3 from the boundary layer (e.g.,
430 Talbot et al., 2005). In the pre-monsoon and monsoon months, the titration is not as strong and
431 the hourly O_3 falls, but generally remains above 10 ppb. Nagarkot, in contrast, is above the
432 valley's boundary layer and has lesser NO for titration at night at this hill station as has been
433 observed in another hill station in Himalayan foothills (Naja and Lal, 2002). Thus, the O_3 level
434 remains above 25 ppb during the entire year at Nagarkot. As also shown in Table 3, at all sites,
435 the O_3 mixing ratios were highest in the pre-monsoon, but the timing of the lowest seasonal
436 values varied across the sites: post-monsoon in Bode, winter in Paknajol and monsoon in
437 Nagarkot. Such differences in minimum O_3 across the sites can be anticipated due to the
438 locations of the sites (e.g., urban, semi-urban, rural and hilltop sites, with differing availabilities
439 of O_3 precursors from different emission sources). The seasonal variations of O_3 observed at
440 Bode in this study are consistent with Putero et al. (2015) and Pudasainee et al. (2006), who also
441 observed O_3 maxima during the pre-monsoon, but O_3 minima during the winter season.
442
443 The daily maximum 8-hour average O_3 mixing ratio (solid colored circles in Figure 6) exceeded
444 the WHO recommended guideline of 50 ppb (WHO, 2006, black dotted line in Figure 6) most
445 frequently during the pre-monsoon period and the winter. During the observation period, the
446 daily maximum 8-hour average O_3 exceeded the WHO guideline on 102 out of 353 days of
447 observation (29%) at Bode, 132/354 days (37%) at Paknajol and 159/357 days (45%) at
448 Nagarkot. The higher exceedance rate at Nagarkot is because it is at higher altitude, which
449 results in (i) greater exposure to large-scale regional pollution, especially from forest fire in the
450 Himalayan foothills and agro residue burning in the IGP region, outside the valley (Sinha et al.,
451 2014, Putero et al., 2015), (ii) less titration of O_3 by NO_x, being farther away from the main

452 pollution sources, and (iii) exposure to O_3 rich free tropospheric air, including influences from
453 stratospheric intrusions. During the SusKat-ABC campaign in 2013 and later in 2014, passive
454 sampling of various gaseous pollutants (SO_2, NO_x, NH_3 and O_3) was also carried out at fourteen
455 sites including urban/semi-urban sites (Bode, Indrachowk, Maharajganj, Mangal Bazar,
456 Suryabinayak, Bhaisepati, Budhanilkantha, Kirtipur, and Lubhu) and rural sites (Bhimdhunga,
457 Naikhandi, Sankhu, Tinpiple, and Nagarkot) in the Kathmandu Valley (Kiros et al., 2016).
458 Similar to this study, they also observed higher O_3 mixing ratios in rural areas than the
459 urban/semi-urban sites in the Kathmandu Valley. Exceedances of the WHO standard are most
460 common during the pre-monsoon season, occurring 78% (72/92 days), 88% (78/89 days) and
461 92% (85/92 days) of the time at Bode, Paknajol and Nagarkot, respectively. Thus, in the context
462 of protecting public health, crops and regional vegetation, the O_3 mixing ratios in the Kathmandu
463 Valley and surrounding areas clearly indicate the urgent need for mitigation action aimed at
464 reducing emissions of its precursor gases NOx and VOCs.
465
466 The SusKat-ABC O_3 data can be compared to observations made about a decade ago by
467 Pudasainee et al. (2006) at the urban site of Pulchowk, not far from Paknajol, as plotted in Figure
468 6d. The daily maximum 8-hour average O_3 had exceeded the WHO guideline at Pulchowk for
469 33% (95/292 days) of days during the observation from November 2003 to October 2004. The
470 exceedance was 38% (133/354 days) of days at Paknajol during Feb 2013 - March 2014. Due to
471 inter-annual variability and differences in the seasonal observation time periods at Pulchowk and
472 Pakanajol, we cannot make any conclusions about trends over the decade between the
473 observations. However, a clear similarity between the observations is that most of the
474 exceedance took place during pre-monsoon season, during which both studies have observations
475 throughout the season (~90 days). The percentage of exceedance at Pulchowk during the pre-
476 monsoon season in 2003-2004 was 70% (63/90 days) and at Pakanajol in 2013 it was 88%
477 (78/89 days). However, like for the annual fraction of exceedances, due to inter-annual
478 variability we cannot say that the 18% (or ca. 15 days) difference in the exceedances is
479 significant. A longer term O_3 record would be needed to really establish if there is a trend in the
480 ozone concentrations.
481
482

Atmos. Chem. Phys. Discuss., https://doi.org/10.5194/acp-2017-709
Manuscript under review for journal Atmos. Chem. Phys.
Discussion started: 18 December 2017

Atmospheric Chemistry and Physics Discussions

3.4 O_3 seasonal and diurnal variation

The seasonal average O_3 mixing ratios at Bode, Nagarkot and Paknajol are shown in Table 3. For comparison, the O_3 mixing ratios measured at two sites in India, (i) Manora Peak (1958 m asl), ca. 9 km from Nainital city, a site in rural mountain setting and (ii) Delhi, a highly-polluted urban setting in northwest IGP are also listed in the Table, based on results from Kumar et al. (2010) and Ghude et al. (2008). There is a strong similarity between the urban and semi-urban sites in Nepal (i.e., Bode, Pakanajol) and India (i.e., Delhi), as well as between the rural and mountain sites in Nepal (i.e., Nagarkot) and India (i.e., Manora Peak), with small differences. The peak mixing ratios were in the pre-monsoon period: at the rural and mountain sites the peak ozone mixing ratio values were very similar (64 and 62 ppb for Nagarkot and Manora Peak, respectively) and are due to influences discussed earlier for Nagarkot; at the sub-urban and urban sites the pre-monsoon values are significantly lower (ca. 40, 42, 33 ppb for Bode, Paknajol, Delhi, respectively) due to fresh NOx emissions near the urban sites and the consequent titration of ozone with NO. The lowest O_3 seasonal values at rural and mountain sites typically occur in the monsoon months while for semi-urban and urban sites, the minimum was observed during post-monsoon (Bode) and winter (Paknajol).

Figure 7 shows the diurnal variation of O_3 mixing ratios at Bode, Paknajol and Nagarkot in the different seasons. The typical O_3 maximum mixing ratio in the early afternoon at the urban and semi-urban sites is mainly due to daytime photochemical production, as well as entrainment of ozone-rich free tropospheric air into the boundary layer, which Putero et al. (2015) suggested results in the broader afternoon peak of ozone during the pre-monsoon at Paknajol site, also observed at Bode site (and somewhat at Nagarkot).

The mixing ratios are relatively constant throughout the day at Nagarkot, which, being a hilltop site, is largely representative of the lower free tropospheric regional pollution values, but is also affected by ozone production from precursors transported from the Kathmandu Valley.

3.5 CO emission flux estimate

It is possible to determine a top-down estimate of the average CO emission flux for the region around the Bode site by applying an approach that was developed and used in Mues et al. (2017) to estimate the emission fluxes of BC at Bode. The analysis of Mues et al. (2017) found BC

fluxes for the Kathmandu Valley that were considerably higher than the widely-used EDGAR HTAP emission database (Version 2.2). Support for this top-down estimate was found by considering the BC concentrations and fluxes for the Kathmandu Valley in comparison to Delhi and Mumbai; although the observed BC concentrations were similar in all three locations, the EDGAR HTAP V2.2 emissions of BC for the Kathmandu Valley are much lower than those for Delhi and Mumbai, while the top-down emissions estimate for the Kathmandu Valley were similar to the emissions from EDGAR HTAP V2.2 for Delhi and Mumbai (Mues et al., 2017).

Here we apply the same method as developed in Mues et al. (2017) to estimate the CO fluxes based on the observed CO mixing ratio and ceilometer observations of the mixing layer height (*MLH*) in Bode for the period of a year (March 2013-February 2014). It is important to note that the term "mixing layer", applied generally to ceilometer observations, is not entirely accurate, since the degree of mixing in the nocturnal stable layer is drastically reduced versus daytime. This adds a degree of uncertainty to the application of ceilometer observations to compute top-down emissions estimates, which will only be resolved once nocturnal vertical profile measurements are also available in order to characterize the nocturnal boundary layer characteristics and the degree to which the surface observations are representative of the mixing ratios throughout the vertical column of the nocturnal stable layer.

Using approach used by Mues et al. (2017), the CO fluxes can be calculated from the increase in CO concentrations during the nighttime period when the *MLH* is nearly constant, using:

$$FCO(t_x, t_y) = \frac{\Delta\mathrm{CO} \times ave(MLH(t_x), MLH\ (t_y))}{\Delta t \times 3600} \times \frac{MLH(t_y)}{MLH\ (t_x)} \quad (1)$$

where $FCO\ (t_x, t_y)$ is the CO emission flux (in µg m^{-2} s^{-1}) between time t_x and t_y (in hours), ΔCO is the change in CO mixing ratio (in µg m^{-3}) between time t_x and t_y, $ave(MLH(t_x), MLH(t_y)$ are average of the mixing layer heights (in m) between time t_x and t_y, Δt is the time interval between t_x and t_y, and $MLH(t_y)/MLH(t_x)$ is mixing layer compression factor, accounting for the small change in MLH during the observation period (see Mues et al., 2017 for details).

Atmos. Chem. Phys. Discuss., https://doi.org/10.5194/acp-2017-709
Manuscript under review for journal Atmos. Chem. Phys.
Discussion started: 18 December 2017

Atmospheric Chemistry and Physics Discussions

This method of calculating the CO emission flux is based on four main assumptions: (i) CO is well-mixed horizontally and vertically within the mixed layer in the region immediately surrounding the Bode site; (ii) the *MLH* remains fairly constant during the night so that the product of the CO concentration (μg m^{-3}) and the *MLH* (m) represents CO mass per unit area within the column, and any change in this represents the net flux into the column; (iii) the transport of air pollutants into and out of the stable nocturnal boundary layer of the valley is negligible, which is supported by the calm winds (<1 m s^{-1}) during the night and morning hours at the site (Mahata et al., 2017); and (iv), the CO emissions during the daytime are similar to those at night, an assumption that is viable on average for some sources like brick kilns which operate day and night, but which does not apply to all sources, e.g., the technique will tend to underestimate emissions due to traffic, which are typically much stronger during the day than at night, while it will overestimate emissions due to waste burning, which is typically more prevalent during the night and early morning (pre-sunrise) than during the daytime. Assumption (iv) is made because equation 1 only works well for calculating the CO flux at night, when there is a relatively constant *MLH* and limited vertical and horizontal mixing. It is not possible to directly compute the emission flux for a full 24-hour day using this top-down method, since the emissions during the day could be either greater or smaller than at night, and because the other assumptions do not hold (in particular there is considerable vertical mixing with the free troposphere and stronger horizontal transport during the daytime). Thus the top-down computation only provides a useful indicative value. However, while it is also not possible to estimate how much different the daytime emissions are, it is possible to determine an absolute lower bound for the CO flux (FCO_{min}) by making the extreme assumption that the CO emissions are non-zero only during the hours which were used in the calculation, and that they were zero during the rest of the day (this provides a lower bound to the emissions since the daytime emissions physically cannot be negative). This lower bound of the flux (FCO_{min}) is thus calculated by scaling back the 24-hour flux to only applying over the calculation time interval (Δt), using:

$$FCO_{min.} = FCO \times \frac{\Delta t}{24} \qquad (2)$$

571 Figure 8 shows the estimated monthly CO emission flux, along with its 25th and 75th percentile
572 values as an indication of the variability of the estimated flux in each month; the lower bound of
573 the CO flux based on Equation 2 is also shown. The estimated annual mean CO flux at Bode is
574 4.92 μg m^{-2} s^{-1}. Seasonally, the emissions are computed to be highest during December to April
575 (3.64-8.36 μg m^{-2} s^{-1}), coinciding with the brick kiln operation period, which resulted in elevated
576 concentrations of most pollutants at Bode (Kim et al., 2015; Chen et al., 2016; Sarkar et al.,
577 2016; Mahata et al., 2017; Mues et al., 2017), including CO (Bhardwaj et al., 2017; Mahata et
578 al., 2017), while the emissions were generally lower during the remaining months (0.54-5.37 μg
579 m^{-2} s^{-1}). The uncertainty in the top-down CO emissions estimate will be largest during June to
580 October, due to the greater diurnal and day-to-day variability with the minimum and maximum
581 CO mixing ratio values during the night and early morning used in Equation 1 often being less
582 distinct than in the other months.
583
584 Comparing the annual mean top-down estimated CO emission flux at Bode (4.92 μg m^{-2} s^{-1}) with
585 available global and regional emission inventories, the top-down estimated CO flux is twice the
586 value, 2.4 μg m^{-2} s^{-1}, for the Kathmandu Valley in the EDGAR HTAP V2.2 emission inventory
587 database for 2010 [note that the CO emission values for the location of Bode and averaged for
588 the valley as a whole (27.65-27.75°N, 85.25-85.40°E) were the same to two significant figures].
589 The estimated CO flux was 6.5-8 times as high as in the REAS database (0.63-0.76 μg m^{-2} s^{-1},
590 based on the 2008 values in Kurokawa et al., 2013), and between 3 and 14 times higher than the
591 values in the INTEX-B database for 2006 (0.35-1.77 μg m^{-2} s^{-1}; Zhang et al., 2009). The large
592 differences between our estimated CO emission flux and these emission databases is not likely to
593 be due to the comparison of data for different years, rather it indicates the substantial
594 uncertainties in both the top-down and bottom-up approaches to estimating the emission flux.
595 Although our approximation of the emission flux relies on several assumptions, the fact that the
596 lower bound value that we calculate is still as high as or higher than the values in some of the
597 published emission datasets likely indicates that the bottom-up emissions are missing or
598 underestimating some important sources, which will be important to examine carefully and
599 improve as a basis for interpreting future modelling studies of CO pollution in the Kathmandu
600 Valley and surrounding regions, as well as for assessing possible mitigation options.
601

4. Conclusions

Ambient CO and O_3 mixing ratios were measured in the framework of the SusKat-ABC international air pollution measurement campaign at five sites (Bode, Paknajol, Bhimdhunga, Naikhandi and Nagarkot) in the Kathmandu Valley (Table 1) and its fringes, initially during January to July 2013, and later extended to one year at three sites (Bode, Paknajol and Nagarkot) to better understand their seasonal characteristics. The observed CO and O_3 levels at all sites except Nagarkot were characteristic of highly-polluted urban settings, with the particular feature that the bowl-shaped valley and resulting meteorology had several effects on the pollution levels.

At all sites, the CO mixing ratios were higher during the early morning and late evening, especially connected to the interplay between the ventilation of the boundary layer and the diurnal cycles of the emission sources. Under calm wind conditions that limited mixing within, into and out of the Kathmandu Valley, the morning CO peak tended to be more pronounced due to the buildup of pollution at night in the shallow planetary boundary layer. This nocturnal buildup was especially strong during January to April at Bode, with the mean CO mixing ratio increasing by about a factor of 4 in the 12 hours from 20:00 to 08:00, especially due to operation of nearby brick kilns continuing through the night. During the daytime, the wind becomes stronger and the horizontal and vertical circulation dilutes and transports pollution around and out of the valley. Although normally the pollution levels are presumed to be higher in the heavily populated valley than in the immediate surrounding region, occasionally the synoptic circulation will transport in CO and O_3-rich air, especially influenced by forest fires and agro-residue burning in the IGP region and Himalayan foothills, as was observed on a few episode days in the pre-monsoon season.

The observed O_3 mixing ratio was highest in the pre-monsoon season at all sites, and the daily maximum 8-hour average O_3 exceeded the WHO guideline of 50 ppb on about 80% of the days during this season at the semi-urban/urban sites of Bode and Paknajol, while at Nagarkot (which is in the free troposphere, i.e., above valley's boundary layer most of the time, especially during nighttime) it exceeded the WHO guideline on 92% of the days in pre-monsoon season. During the whole observation period, the 8 hour maximum average O_3 exceeded the WHO recommended value on 29%, 37% and 45% of the days at Bode, Paknajol and Nagarkot, respectively. The diurnal cycle showed evidence of photochemical production as well as possible

down-mixing of O_3 during the daytime, with the hourly mixing ratio at the polluted site increasing from typically 5-20 ppb in the morning to an early afternoon peak of 60-120 ppb.

These high O_3 levels have deleterious effects on human health and ecosystems, including agro-ecosystems in the Kathmandu Valley and surrounding regions, thus justifying mitigation measures to help reduce the levels of O_3 (its precursors VOCs and NOx), CO and other pollutants. Determining the most effective mitigation measures will be challenging due to the complicated interplay of pollution and meteorology as well as local and regional pollution sources. This study has provided information on current ambient levels and the diurnal/seasonal variations. This will be helpful in the design of future policies, both as a baseline for evaluating the effectiveness of mitigation measures, as well as giving insight into the connections between various pollutant sources (e.g., brick kilns) and their impacts on seasonally elevated CO levels, especially at nighttime. One particular contribution has been the development of a top-down estimate of the total emission flux of CO at Bode, which was found to be 4.92 $\mu g\ m^{-2}\ s^{-1}$. This is several times higher (by a factor of 2-14 times) than the CO emission fluxes for the Kathmandu Valley in state-of-the-art inventories such as EDGAR-HTAP, REAS, and INTEX-B. This points out the need for the development of updated comprehensive emission inventory databases for this region, in order to provide more accurate input to model simulations needed to assess air pollution processes and mitigation options for the Kathmandu Valley and the broader surrounding region.

While the high levels of particulate pollution in the Kathmandu Valley have caught the main attention of the public and policymakers, due to their immediately visible nature, our paper points out that ozone is also a serious problem here. In fact, its higher levels on the nearby mountaintop location of Nagarkot, which is much more representative of regional air pollution, point to an ozone problem in the wider foothills of the Himalayas that the extent of ozone pollution in the large surrounding Himalayan foothills has been insufficiently recognized until our study, and that needs monitoring and research to identify feasible mitigation options.

Acknowledgement

We are thankful to the funders of the IASS – the German Ministry of Education and Research (BMBF) and the Brandenburg State Ministry of Science, Research and Culture (MWFK) – for their generous support in making these measurements and their analysis possible. This study was partially supported by core funds of ICIMOD contributed by the governments of Afghanistan, Australia, Austria, Bangladesh, Bhutan, China, India, Myanmar, Nepal, Norway, Pakistan, Switzerland, and the United Kingdom, as well as by funds from the Government of Sweden to ICIMOD's Atmosphere Initiative. The authors would like to thank Bhupesh Adhikary, Bhogendra Kathayat, Shyam Newar, Dipesh Rupakheti, Nirjala Koirala, Ashish Bhatta, Begam Roka, Sunil Babu Khatry, Giampietro Verza, and several staff members at the Kamdhenu Madhyamik Vidhyalaya, Naikhandi who assisted in the field measurements, Siva Praveen Puppala for initial data processing, and Pankaj Sadavarte for helping with the emission databases. We are grateful to the Department of Environmental Sciences, University of Virginia, USA, for making available CO and O_3 instruments for the measurements. We also thank the staff at Real Time Solutions (RTS), Lalitpur, Nepal for providing an automatic weather station.

References

Avnery, S., Mauzerall, D. L., Liu, J., and Horowitz, L. W.: Global crop yield reductions due to surface ozone exposure: 1. Year 2000 crop production losses and economic damage, Atmos. Environ., 45, 2284–2296, doi:10.1016/j.atmosenv.2010.11.045, 2011.

Bhardwaj, P., Naja, M., Rupakheti, M., Panday, A. K., Kumar, R., Mahata, K., Lal, S., Lawrence, M. G., Chandola, H. C.: Variations in surface ozone and CO in the Kathmandu Valley during SusKat-ABC international field campaign, Atmos. Chem. Phys. Discus., https://doi.org/10.5194/acp-2017-306, 2017.

Bonasoni P., P. Laj, A. Marinoni, M. Sprenger, F. Angelini, J. Arduini, U. Bonafè, F. Calzolari, T. Colombo, S. Decesari, C. Di Biagio, A. G. di Sarra, et. al.: Atmospheric brown clouds in the Himalayas: first two years of continuous observations at the Nepal Climate Observatory-Pyramid (5079 m). Atmos. Chem. Phys., 10, 7515-7531, 2010.

690 Brauer, M., Amman, M., Burnett, R. T., Cohen, A., Dentener, F., Zenati, M., Henderson, S. B.,
691 Krzyzanowski, M., Martin, R. V., Van Dingenen, R., van Donkelaar, A., and Thurston, G. D.:
692 Exposure assessment for estimation of the global burden of disease attributable to outdoor air
693 pollution, Environ. Sci. Technol., 46, 652–660, doi:10.1021/es2025752, 2012.

694 Burney, J., and Ramanathan, V.: Recent climate and air pollution impacts on Indian agriculture,
695 Proceedings of the National Academy of Sciences of the United States of America, 111, 16319-
696 16324, doi:10.1073/pnas.1317275111, 2014.

697 Chen, P., Kang, S., Li, C., Rupakheti, M., Yan, F., Li, Q., Ji, Z., Zhang, Q., Luo, W., Sillanpää,
698 M.: Characteristics and sources of polycyclic aromatic hydrocarbons in atmospheric aerosols in
699 the Kathmandu Valley, Nepal, Sci. Total Environ., 538, 86-92, doi:
700 10.1016/j.scitotenv.2015.08.006, 2015.

701 Cristofanelli, P., Bracci, A., Sprenger, M., Marinoni, A., Bonafè, U., Calzolari, F., Duchi, R.,
702 Laj, P., Pichon, J. M., Roccato, F., Venzac, H., Vuillermoz, E., and Bonasoni, P.: Tropospheric
703 ozone variations at the Nepal Climate Observatory- Pyramid (Himalayas, 5079ma.s.l.) and
704 influence of deep stratospheric intrusion events, Atmos. Chem. Phys., 10, 6537–6549,
705 doi:10.5194/acp-10-6537-2010, 2010.

706 Dentener, F., Stevenson, D., Ellingsen, K., Van Noije, T., Schultz, M., Amann, M., Atherton, C.,
707 Bell, N., Bergmann, D., and Bey, I.: The global atmospheric environment for the next
708 generation, Environ. Sci. Technol., 40, 3586-3594, 2006.

709 Davidson, C. I., Lin, S.-F., and Osborn, J. F.: Indoor and outdoor air pollution in the Himalayas,
710 Environ. Sci. Technol., 20(6), 561 – 566, doi:10.1021/es00148a003, 1986.

711 Dhungel, S., Kathayat, B., Mahata, K., and Panday, A.: Transport of regional pollutants through
712 a remote trans-Himalayan valley in Nepal, Atmos. Chem. Phys. Discuss., 2016, 1-23,
713 doi:10.5194/acp-2016-824, 2016.

714 Department of Transport Management (DoTM).: Annual report of Ministry of Labor and
715 Transport Management, Government of Nepal, 2015.

716 Forouzanfar, M. H., Alexander, L., Anderson, H. R., Bachman, V. F., Biryukov, S., Brauer, M.,
717 Burnett, R., Casey, D., Coates, M. M., and Cohen, A.: Global, regional, and national comparative
718 risk assessment of 79 behavioural, environmental and occupational, and metabolic risks or
719 clusters of risks in 188 countries, 1990–2013: a systematic analysis for the global burden of
720 disease study 2013, Lancet, 386, 2287-2323, doi: 10.1016/S0140-6736(15)00128-2, 2015.

721 Fowler, D., Flechard, C., Cape, J. N., Storeton-West, R. L., and Coyle, M.: Measurements of
722 ozone deposition to vegetation quantifying the flux, the stomatal and nonstomatal components,
723 Water Air Soil Pollut., 130, 63–74, doi:10.1023/a:1012243317471, 2001.

724 Geiß, A., Wiegner, M., Bonn, B., Schäfer, K., Forkel, R., von Schneidemesser, E., Münkel, C.,
725 Chan, K. L., and Nothard, R.: Mixing layer height as an indicator for urban air quality?, Atmos.
726 Meas. Tech. Discuss., 2017, 1-32, doi:10.5194/amt-2017-53, 2017.

727 Giri, D., Murthy, K., Adhikary, P., Khanal, S.: Ambient air quality of Kathmandu Valley as
728 reflected by atmospheric particulate matter concentrations (PM10), Int. J. Environ. Sci. Technol.
729 3, 403–410, 2006.

730 International Energy Agency (IEA).: Energy and air pollution, World Energy Outlook Special
731 Report 2016, International Energy Agency, 2016.

732 Janssens-Maenhout, G., Dentener, F., van Aardenne, J., Monni, S., Pagliari, V., Orlandini, L.,
733 Klimont, Z., Kurokawa, J., Akimoto, H., Ohara, T., Wankmüller, R., Battye, B., Grano, D.,
734 Zuber, A., and Keating, T.: EDGAR-HTAP: a harmonized gridded air pollution emission dataset
735 based on national inventories, Tech. Rep. JRC68434, Publications Office of the European Union,
736 doi:10.2788/14102 (online), http://publications.jrc.ec.europa.eu/repository/handle/JRC68434,
737 2000.

738 Kiros, F., Shakya, K. M., Rupakheti, M., Regmi, R. P., Maharjan, R., Byanju, R. M., Naja, M.,
739 Mahata, K., Kathayat, B., and Peltier, R. E.: Variability of Anthropogenic Gases: Nitrogen
740 oxides, sulfur dioxide, ozone and ammonia in Kathmandu Valley, Nepal, Aerosol Air Qual. Res.,
741 16: 3088–3101, 2016.

742 Kumar, R., Naja, M., Venkataramani, S., and Wild, O.: Variation in surface ozone at Nainital: A
743 high-altitude site in the central Himalayas, J. Geophys. Res., 115 (D16),
744 doi:10.1029/2009JD013715, 2010.

745 Kurokawa, J., Ohara, T., Morikawa, T., Hanayama, S., Janssens-Maenhout, G., Fukui, T.,
746 Kawashima, K., and Akimoto, H.: Emissions of air pollutants and greenhouse gases over Asian
747 regions during 2000-2008: Regional emission inventory in Asia (REAS) version 2, Atmos.
748 Chem. Phys., 13, 11 019–11 058, doi:10.5194/acp-13-11019-2013, 2013.

749 Lawrence, M., and Lelieveld, J.: Atmospheric pollutant outflow from southern Asia: a review,
750 Atmos. Chem. Phys., 10, 11017-11096, 2010.

751 Lim, S. S., Vos, T., Flaxman, A. D., Danaei, G., Shibuya, K., Adair-Rohani, H., Amann, M.,
752 Anderson, H. R., Andrews, K. G., Aryee, M., Atkinson, C., Bacchus, L. J., Bahalim, A. N.,
753 Balakrishnan, K., Balmes, J., Barker-Collo, S., Baxter, A., Bell, M. L., Blore, J. D., Blyth, F.,
754 Bonner, C., Borges, G., Bourne, R…and Ezzati, M.: A comparative risk assessment of burden of
755 disease and injury attributable to 67 risk factors and risk factor clusters in 21 regions, 1990-2010:
756 a systematic analysis for the global burden of disease study 2010, Lancet, 380, 2224–2260, 2012.

757 Lüthi, Z. L., Škerlak, B., Kim, S. W., Lauer, A., Mues, A., Rupakheti, M., and Kang, S.:
758 Atmospheric brown clouds reach the Tibetan Plateau by crossing the Himalayas, Atmos. Chem.
759 Phys. 15, 6007-6021, doi:10.5194/acp-15-6007-2015, 2015.

760 Mahata, K. S., Panday, A. K., Rupakheti, M., Singh, A., Naja, M., and Lawrence, M. G.:
761 Seasonal and diurnal variations of methane and carbon dioxide in the Kathmandu Valley in the
762 foothills of the central Himalaya, Atmos. Chem. Phys. Discuss., 2017, 1-55, doi:10.5194/acp-
763 2016-1136, 2017.

764 Marinoni, A., Cristofanelli, P., Laj, P., Duchi., R., Putero, D., Calzolari, F., Landi., T. C.,
765 Vuillermoz, E., Maione, M., and Bonasoni, P.: High black carbon and ozone concentrations
766 during pollution transport in the Himalayas: Five years of continuous observations at NCO-P
767 global GAW station, J. Environ. Sci., 25(8) 1618–1625, 2013.

768 Ming, J., Xiao, C., Sun, J., Kang, S.-C, and Bonasoni, P.: Carbonaceous particles in the
769 atmosphere and precipitation of the Nam Co region, central Tibet, J. Environ. Sci.-CHINA,
770 22(11), 1748-1756, 2010.

771 Monks, P. S., Granier, C., Fuzzi, S., Stohl, A., Williams, M. L., Akimoto, H., Amann, M.,
772 Baklanov, A., Baltensperger, U., Bey, I., Blake, N., Blake, R. S., Carslaw, K., Cooper, O. R.,
773 Dentener, F., Fowler, D., Fragkou, E., Frost, G. J., Generoso, S., Ginoux, P., Grewe, V.,
774 Guenther, A., Hansson, H. C., Henne, S., Hjorth, J., Hofzumahaus, A., Huntrieser, H., Isaksen, I.
775 S. A., Jenkin, M. E., Kaiser, J., Kanakidou, M., Klimont, Z., Kulmala, M., Laj, P., Lawrence, M.
776 G., Lee, J. D., Liousse, C., Maione, M., McFiggans, G., Metzger, A., Mieville, A.,
777 Moussiopoulos, N., Orlando, J. J., O'Dowd, C. D., Palmer, P. I., Parrish, D. D., Petzold, A.,
778 Platt, U., Poeschl, U., Prevot, A. S. H., Reeves, C. E., Reimann, S., Rudich, Y., Sellegri, K.,
779 Steinbrecher, R., Simpson, D., ten Brink, H., Theloke, J., van derWerf, G. R., Vautard, R.,
780 Vestreng, V., Vlachokostas, C., and von Glasow, R.: Atmospheric composition change – global
781 and regional air quality, Atmos. Environ., 43, 5268–5350, doi:10.1016/j.atmosenv.2009.08.021,
782 2009.

783 Naja, M., and Lal, S.: Surface ozone and precursor gases at Gadanki (13.5°N, 79.2°E), a tropical
784 rural site in India, J. Geophys. Res. 107 (D14), ACH 8-1-ACH 8–13, doi:10.1029/2001jd000357,
785 2002.

786 Nayava, J. L.: Rainfall in Nepal, the Himalayan Rev. Nepal, Geographical Society, 12:1– 18,
787 1980.

788 Organisation for Economic Co-operation and Development (OECD): The economic
789 consequences of outdoor air pollution, OECD Publishing,
790 doi: http://dx.doi.org/10.1787/9789264257474-en, 2016.

791 Panday, A. K., and Prinn, R. G..: Diurnal cycle of air pollution in the Kathmandu Valley, Nepal:
792 Observations, J. Geophys. Res., 114 (D9), doi:10.1029/2008JD009777, 2009.

793 Panday, A. K. Prinn, R. G., and Schär, C.: Diurnal cycle of air pollution in the Kathmandu
794 Valley, Nepal: 2. Modeling results, J. Geophys. Res., 114 (D21), doi:10.1029/2008JD009808,
795 2009.

796 Pudasainee, D., Sapkota, B., Shrestha, M. L., Kaga, A., Kondo, A., and Inoue, Y.: Ground level
797 ozone concentrations and its association with NOx and meteorological parameters in Kathmandu
798 Valley, Nepal, Atmos. Environ., 40(40), 8081–8087, doi:10.1016/j.atmosenv.2006.07.011, 2006.

799 Putero, D., Cristofanelli, P., Marinoni, A., Adhikary, B., Duchi, R., Shrestha, S.D., Verza, G.P.,
800 Landi, T.C., Calzolari, F., Busetto, M., Agrillo, G., Biancofiore, F., Di Carlo, P., Panday, A. K.,
801 Rupakheti, M., and Bonasoni,P.: Seasonal variation of ozone and black carbon observed at
802 Paknajol, an urban site in the Kathmandu Valley, Nepal. Atmos. Chem. Phys., 15(24), 13957-
803 13971, doi:10.5194/acp-15-13957-2015, 2015.

804 Ram, K., and Sarin, M.: Spatio-temporal variability in atmospheric abundances of EC, OC and
805 WSOC over Northern India, J. Aerosol Sci., 41, 88–98, 2010.

806 Regmi, R. P., Kitada, T., and Kurata, G.: Numerical simulation of late wintertime local flows in
807 Kathmandu Valley, Nepal: Implication for air pollution transport, J. Appl. Meteorol., 42, 389-
808 403, 2003.

809 Rupakheti, M., Panday, A. K., Lawrence, M. G., Kim, S. W., Sinha, V., Kang, S. C., Naja, M.,
810 Park, J. S., Hoor, P., Holben, B., Sharma, R. K., Mues, A., Mahata, K. S., Bhardwaj, P., Sarkar,
811 C., Rupakheti, D., Regmi, R. P., and Gustafsson, Ö.: Air pollution in the Himalayan foothills:
812 overview of the SusKat-ABC international air pollution measurement campaign in Nepal,
813 Atmos. Chem. Phys. Discuss., in preparation, 2017.

814 Rupakheti, D., Adhikary, B., Praveen, P. S., Rupakheti, M., Kang, S.-C., Mahata, K. S., Naja,
815 M., Zhang, Q., Panday, A. K., and Lawrence, M. G.: Pre-monsoon air quality over Lumbini, a
816 world heritage site along the Himalayan foothills, Atmos. Chem. Phys., 17, 11041-11063,
817 https://doi.org/10.5194/acp-17-11041-2017, 2017.

818 Sarkar, C., Sinha, V., Kumar, V., Rupakheti, M., Panday, A., Mahata, K.S., Rupakheti, D.,
819 Kathayat, B., and Lawrence, M.G.: Overview of VOC emissions and chemistry from PTR-TOF-
820 MS measurements during the SusKat-ABC campaign: high acetaldehyde, isoprene and isocyanic
821 acid in wintertime air of the Kathmandu Valley, Atmos. Chem. Phys., 16, 3979-4003, 2016.

822 Sarkar, C., Sinha, V., Sinha, B., Panday, A. K., Rupakheti, M., and Lawrence, M. G.: Source
823 apportionment of NMVOCs in the Kathmandu Valley during the SusKat-ABC international field
824 campaign using positive matrix factorization, Atmos. Chem. Phys., 17, 8129-8156, 2017.

825 Shakya, K. M., Rupakheti, M., Shahi, A., Maskey, R., Pradhan, B., Panday, A., Puppala, S. P.,
826 Lawrence, M., and Peltier, R. E.: Near-road sampling of PM2. 5, BC, and fine-particle chemical
827 components in Kathmandu Valley, Nepal, Atmos. Chem. Phys., 17, 6503-6516,
828 https://doi.org/10.5194/acp-17-6503-2017, 2017.

829 Shrestha, A. B., Wake, C. P., Mayewski, P. A., and Dibb, J.E.: Maximum Temperature Trends in
830 the Himalaya and Its Vicinity: An Analysis Based on Temperature Records from Nepal for the
831 Period 1971–94, J. Climate, 12, 2775-2786, 1999.

832 Shrestha, S. R., Kim Oanh, N. T., Xu, Q., Rupakheti, M., and Lawrence, M. G.: Analysis of the
833 vehicle fleet in the Kathmandu Valley for estimation of environment and climate co-benefits of
834 technology intrusions, Atmos. Environ., 81, 579-590, 2013.

835 Silva, R. A., West, J. J., Zhang, Y., Anenberg, S. C., Lamarque, J.-F., Shindell, D. T., Collins,
836 W. J., Dalsoren, S., Faluvegi, G., Folberth, G., Horowitz, L. W., Nagashima, T., Naik, V.,
837 Rumbold, S., Skeie, R., Sudo, K., Takemura, T., Bergmann, D., Cameron- Smith, P., Cionni, I.,
838 Doherty, R. M., Eyring, V., Josse, B., MacKenzie, I. A., Plummer, D., Righi, M., Stevenson, D.
839 S., Strode, S., Szopa, S., and Zeng, G.: Global premature mortality due to anthropogenic outdoor
840 air pollution and the contribution of past climate change, Environ. Res. Lett., 8, 034005,
841 doi:10.1088/1748-9326/8/3/034005, 2013.

842 Talbot, R., Mao, H., and Sive, B.: Diurnal characteristics of surface level O_3 and other important
843 trace gases in New England, J. Geophys. Res., 110 (D9), doi:10.1029/2004JD005449, 2005.

844 Tripathee, L., Kang, S.-C., Huang, J., Sharma, C., Sillanpaa, M., Guo, J., and Paudyal, R.:
845 Concentrations of trace elements in wet deposition over the central Himalayas, Nepal, Atmos.
846 Environ., 95, 231–238, 2014

847 Sinha, V., Kumar, V., and Sarkar, C.: Chemical composition of pre-monsoon air in the Indo-
848 Gangetic Plain measured using a new air quality facility and PTR-MS: high surface ozone and

849 strong influence of biomass burning, Atmos. Chem. Phys., 14, 5921-5941, doi:10.5194/acp-14-
850 5921-2014, 2014.

851 Vadrevu, K., Ellicott, E., Giglio, L., Badarinath, K., Vermote, E., Justice, C., Lau, W.:
852 Vegetation fires in the Himalayan region - aerosol load, black carbon emissions and smoke
853 plume heights, Atmos. Environ., 47, 241–251, 2012.

854 World Health Organization (WHO): WHO Air quality guidelines for particulate matter, ozone,
855 nitrogen dioxide and sulfur dioxide, Global update 2005, Summary of risk assessment, WHO
856 Press, Geneva, Switzerland, 2006.

857 World Health Organization (WHO).: 7 million premature deaths annually linked to air pollution,
858 2014 (http://www.who.int/mediacentre/news/releases/2014/air-pollution/en/)

859 Zhang, Q., Streets, D., Carmichael, G., He, K., Huo, H., Kannari, A., Klimont, Z., Park, I.,
860 Reddy, S., Fu, J., Chen, D., Duan, L., Lei, Y., Wang, L., and Yao, Z.: Asian emissions in 2006
861 for the NASA INTEX-B mission, Atmos. Chem. Phys., 9, 5131–5153, 2009.

862

Atmos. Chem. Phys. Discuss., https://doi.org/10.5194/acp-2017-709
Manuscript under review for journal Atmos. Chem. Phys.
Discussion started: 18 December 2017

Atmospheric Chemistry and Physics Discussions

Table 1. Information on the sampling sites (of the SusKat-ABC campaign) used in this study with sampling carried out during 2013-2014 in the Kathmandu Valley. The altitude is in meter above mean sea level (m asl)

Site	General setting of site	Location, altitude (m asl)
Bode	Sub-urban, tallest building with scattered houses surrounded by agricultural fields	27.69°N, 85.40°E, 1345
Bhimdhunga	Rural. On the ridge, close to the pass separating the Kathmandu Valley from a valley of a tributary the Trishuli River to the west	27.73°N, 85.23°E, 1522
Paknajol	Urban, city-center, the tallest building in the neighborhood	27.72°N, 85.30°E, 1380
Naikhandi	Rural, at outlet of Bagmati River in Southwest corner of the Valley	27.60°N, 85.29°E, 1233
Nagarkot	Mountain rural. Mountain top site of the eastern valley rim, north facing towards the Kathmandu Valley	27.72°N , 85.52°E, 1901

Atmos. Chem. Phys. Discuss., https://doi.org/10.5194/acp-2017-709
Manuscript under review for journal Atmos. Chem. Phys.
Discussion started: 18 December 2017

Atmospheric Chemistry and Physics Discussions

Table 2. Details of the instruments deployed at different sites during the observation period during January 2013-March 2014 in the Kathmandu Valley.

Location	Instrument	Parameters	Inlet/sensor height (above ground)	Duration	Group
1. Bode	a. Horiba APMA-370	CO	20 m	1 Jan-7 Jun 2013	ARIES
	b. Teledyne 400E	O_3	20 m	1 Jan-7 Jun 2013	ARIES
	c. Thermo Scientific 49i	O_3	20 m	18 Jun-31 Dec 2013	IASS
	d. Picarro G2401	CO	20 m	6 Mar 2013-5 Mar 2014	ICIMOD
	e. Campbell AWS	T, RH, SR, WS, WD, RF	22 m	1 Jan-30 Mar 2013	IASS
	f. Davis AWS (Vantage Pro2)	T, RH, P, RF	21 m	30 May-Jul 2013	UVA
	g. Ceilometer (Vaisala CL31)	MLH	20 m	01 Mar 2013- 28 Feb 2014	JGUM
2. Bhimdhunga	a. Thermo Scientific 48i	CO	2 m	1 Jan-15 Jul 2013	UVA
	b. AWS Hobo Onset	T, RH, SR, WS, WD, P	5 m	1 Jan-30 Jun 2013	UVA
3. Naikhandi	a. Thermo Scientific 48i	CO	5 m	3 Jan- 6 Jun 2013	UVA
	b. 2B Tech. Model 205	O_3	5 m	1 Feb-25 May 2013	UVA
	c. AWS Hobo Onset	T, RH, SR, WS, WD, P	2 m	3 Jan-25 Apr 2013	UVA
4. Nagarkot	a. Thermo Scientific 48i	CO	5 m	13 Feb-Apr 3 2013; 8 Jun-15 Jul 2013	UVA
	b. Thermo Scientific 49i	O_3	5 m	9 Jan-30 Jun 2013	UVA
	c. Campbell AWS	T, RH, SR, WS, WD, RF	7 m		IASS
	d. AWS (Vaisala WXT 520)	T, RH, SR, WS, WD, RF, P	7 m	10 Feb-30 Jun 2013	RTS
5. Paknajol	a. Thermo Environmental (49i)	O_3	25 m	1 Feb 2013-30 Jan 2014	EV-K2-CNR
	b. AWS (Vaisala WXT 425)	T, RH, SR, WS, WD, RF, P	25 m	1 Feb 2013-30 Jan 2014	EV-K2-CNR

Note: T - temperature, RH - relative humidity, SR- solar radiation, WS - wind speed, WD - wind direction, RF- rainfall, P – pressure and MLH – Mixing layer height; ARIES - Aryabhatta Research Institute of Observational Sciences, India; ICIMOD - International Center for Integrated Mountain Development, Nepal; IASS - Institute for Advanced Sustainability Studies, Germany; UVA- University of Virginia, USA; JGUM – Johannes Gutenberg University Mainz, Germany; RTS - Real Time Solutions, Nepal; Ev-K2-CNR - Everest-Karakorum - Italian National Research Council, Italy.

Atmos. Chem. Phys. Discuss., https://doi.org/10.5194/acp-2017-709
Manuscript under review for journal Atmos. Chem. Phys.
Discussion started: 18 December 2017

Atmospheric Chemistry and Physics Discussions

Table 3. Summary of the monthly average ozone mixing ratios (ppb) [average (Avg), standard deviation (SD), minimum (Min.) and maximum (Max.)] at four sites* in the Kathmandu Valley, Nepal during 2013-2014 and two sites (Manora Peak and Delhi) in India

	Bode	Paknajol	Nagarkot	Manora[a] Peak	Delhi[b]
Month	Avg ± SD [Min., Max.]	Avg ± SD [Min., Max.]	Avg ± SD [Min., Max.]	Avg ± SD	Avg [Min., Max.]
January	23.5 ± 19.9 [1.4, 87.1]	16.9 ± 18.3 [0.1, 71.7]*	46.7 ± 5.7 [36.4, 73.7	37.3 ± 14.8	19.3 [10, 14.7]
February	25.6 ± 20.4 [1.2, 94.5]	24.2± 20.1 [1.6, 91.7]	47.5 ± 7.5 [28.2, 83.6]	43.8 ± 16.8	25.3 [10.9, 55.7]
March	37.4 ± 24.3 [1.2, 105.9]	37.7 ± 23.8 [1.6, 95.8]	62.4 ± 9.5 [40.5, 98.9]	56.6 ± 11.4	29.7 [13.8, 58]
April	43.4 ± 26.6 [1.4, 116.2]	46.7 ± 26.8 [1.0, 115.5]	71.5 ± 15.5 [40.1, 121.0]	63.1 ± 11.7	33 [13.7, 64.3]
May	38.5 ± 21.2 [2.0, 111.1]	42.8 ± 20.6 [6.7, 103.3]	59.0 ± 20.6 [15,0, 124.5]	67.2 ± 14.2	35.4 [19.8, 62]
June	27.8 ± 12.0 [1.7, 68.4]	27.5 ± 17.0 [0.6, 90.7]	34.2 ± 9.1 [4.6, 72.0]	44.0 ± 19.5	25.6 [12.8, 46.4]
July	21.1 ± 9.5 [1.7, 82.0]	20.5 ± 13.4 [2.0, 77.9]	25.9 ± 6.2 [11.1, 48.0]	30.3 ± 9.9	19.1 [9.4, 37.1]
August	20.3 ± 9.9 [2.0, 70.9]	20.1 ± 12.6 [0.8, 73.1]	28.3 ± 5.8 [15.5, 62.9]	24.9 ± 8.4	14.3 [9.7, 29.5]
September	23.3 ± 14.9 [0.5, 85.9]	24.9 ± 17.4 [0.4, 108.1]	34.8 ± 9.6 [16.1, 79.7]	32.0 ± 9.1	17.7 [7.7, 37.7]
October	19.4 ± 13.8 [0.1, 70.9]	22.6 ± 17.0 [0.6, 83.5]	35.2 ± 10.2 [18.0, 73.8]	42.4 ± 7.9	21.7 [9, 56.9]
November	18.6 ± 15.1 [0.3, 67.7]	22.4 ± 20.9 [0.1, 84.0]	40.1 ± 8.1 [25.6, 73.3]	43.9 ± 7.6	22.6 [9, 55.1]
December	21.7 ± 17.8 [1.0, 96.6]	19.5 ± 19.7 [0.1, 82.0]	43.8 ± 9.0 [24.8, 85.11]	41.6 ± 6.3	20.2 [9.1, 40.3]
Season:					
Winter	24.5 ± 20.1 [1.2, 94.5]	20.2 ± 19.6 [0.1, 91.7]	45.8 ± 7.8 [24.8, 85.1]	40.9	21.6 [9.1, 55.7]
Pre-monsoon	39.8 ± 24.2 [1.2, 116.2]	42.4 ± 24.0 [1.0, 115.5]	64.3 ± 16.7 [14,9, 124.5]	62.3	32.7 [13.7, 64.3]
Monsoon	22.7 ± 12.0 [0.5, 85.9]	23.2 ± 15.5 [0.4, 108.1]	30.8 ± 8.7 [4.6, 79.7]	32.8	19.2 [7.7, 46.4]
Post-monsoon	19.0 ± 14.5 [0.1, 70.9]	22.5 ± 18.9 [0.1, 84.0]	37.6 ± 9.5 [18.0, 73.8]	39.4	22.2 [9, 56.9]

[a] Kumar et al. (2010), [b] Ghude et al. (2008). * O_3 data of Paknajol on January was of 2014.

Atmos. Chem. Phys. Discuss., https://doi.org/10.5194/acp-2017-709
Manuscript under review for journal Atmos. Chem. Phys.
Discussion started: 18 December 2017

Atmospheric Chemistry and Physics Discussions

Table 4. Averege CO mixing ratio (ppb) at different time of the day (daytime - 12:00 – 16:00), and nighttime - 23:00 – 03:00) and the monthly average (total) at four sites in the Kathmandu Valley.

	Winter (16 Jan-15 Feb)			Pre-monsoon (16 Mar-15 Apr)			Monsoon (16 Jun-15Jul)			Post-monsoon (16 Oct-15 Nov)		
Sites	daytime	nighttime	total	daytime	nighttime	total	daytime	nighttime	total	daytime	nighttime	total
Bode	405.35	927.21	819.17	430.91	839.17	770.52	210.59	230.08	241.34	269.10	453.95	397.24
Bhimdhunga	324.62	354.23	374.27	374.64	479.37	471.33	196.61	202.85	198.40			
Naikhandi	280.97	356.14	380.40	382.71	425.17	449.83						
Nagarkot							141.68	158.78	160.41			

Atmos. Chem. Phys. Discuss., https://doi.org/10.5194/acp-2017-709
Manuscript under review for journal Atmos. Chem. Phys.
Discussion started: 18 December 2017

Atmospheric Chemistry and Physics Discussions

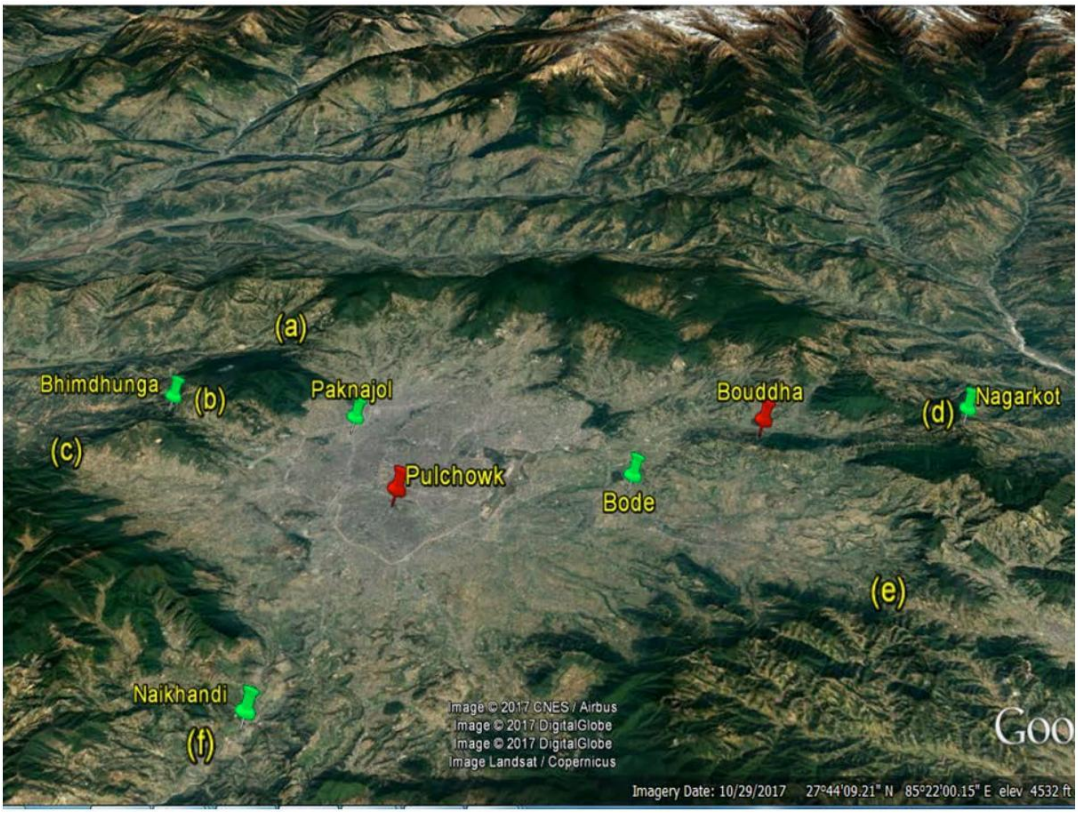

Figure 1. Observation sites in the SusKat-ABC international air pollution campaign during 2013-2014 in the Kathmandu Valley. Bode, Paknajol, and Naikhandi were selected within the valley floor and Bhimdhunga and Nagarkot on the mountain ridge. Naikhandi site is also near the Bagmati River outlet. Major passes of the Kathmandu Valley are (a) Mudku Bhanjhyang pass, (b) Bhimdhunga pass and (c) Nagdhunga pass in the west, and (d) Nagarkot and (e) Nala pass in the east and only (f) river outlet in the valley are shown in the Figure. Past study sites (Bouddha and Pulchowk), which are referred in the manuscript, are also shown in the Figure. Source: Google Earth.

Atmos. Chem. Phys. Discuss., https://doi.org/10.5194/acp-2017-709
Manuscript under review for journal Atmos. Chem. Phys.
Discussion started: 18 December 2017

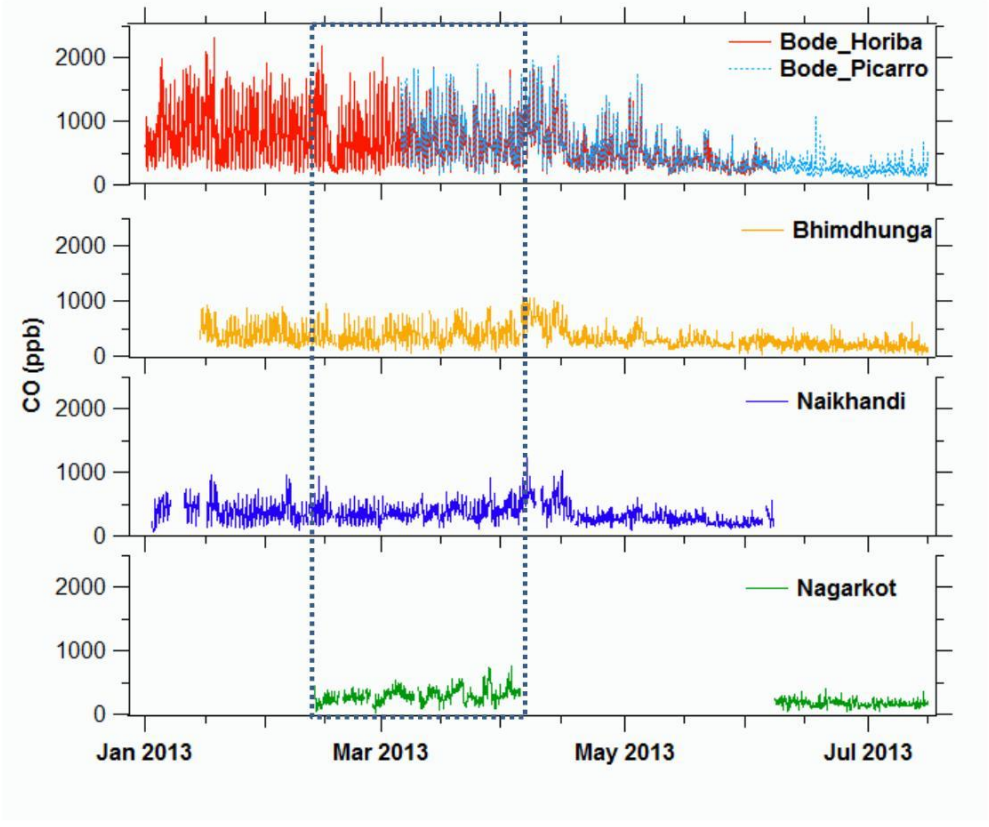

Figure 2. Hourly average CO mixing ratios observed at supersite (Bode) and three satellite sites (Bhimdhunga, Naikhandi and Nagarkot) of the SusKat-ABC international air pollution measurement campaign during January to July 2013 in the Kathmandu Valley. The dotted box represents a period (13 February - 03 April, 2013) during which data for all four sites were available.

Atmos. Chem. Phys. Discuss., https://doi.org/10.5194/acp-2017-709
Manuscript under review for journal Atmos. Chem. Phys.
Discussion started: 18 December 2017

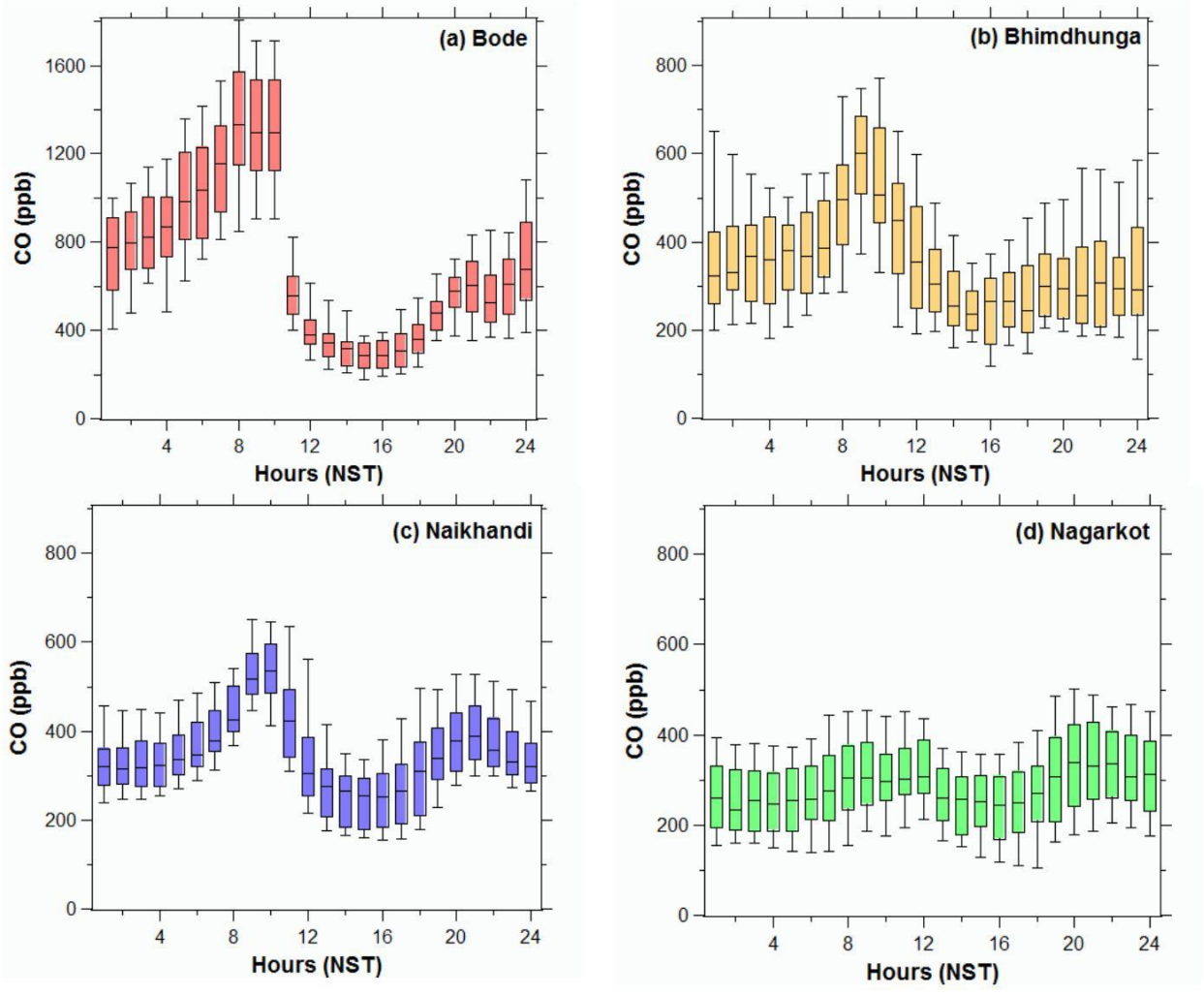

Figure 3. Diurnal variations of hourly average CO mixing ratios during the common observation period (13 February–03 April, 2013) at Bode, Bhimdhunga, Naikhandi and Nagarkot. The lower end and upper end of the whisker represents 10th and 90th percentile, respectively; the lower end and upper end of each box represents the 25th and 75th percentile, respectively, and the black horizontal line in the middle of each box is the median for each month. Note: the y-axis scale of Bode is twice that of the three sites.

Atmos. Chem. Phys. Discuss., https://doi.org/10.5194/acp-2017-709
Manuscript under review for journal Atmos. Chem. Phys.
Discussion started: 18 December 2017

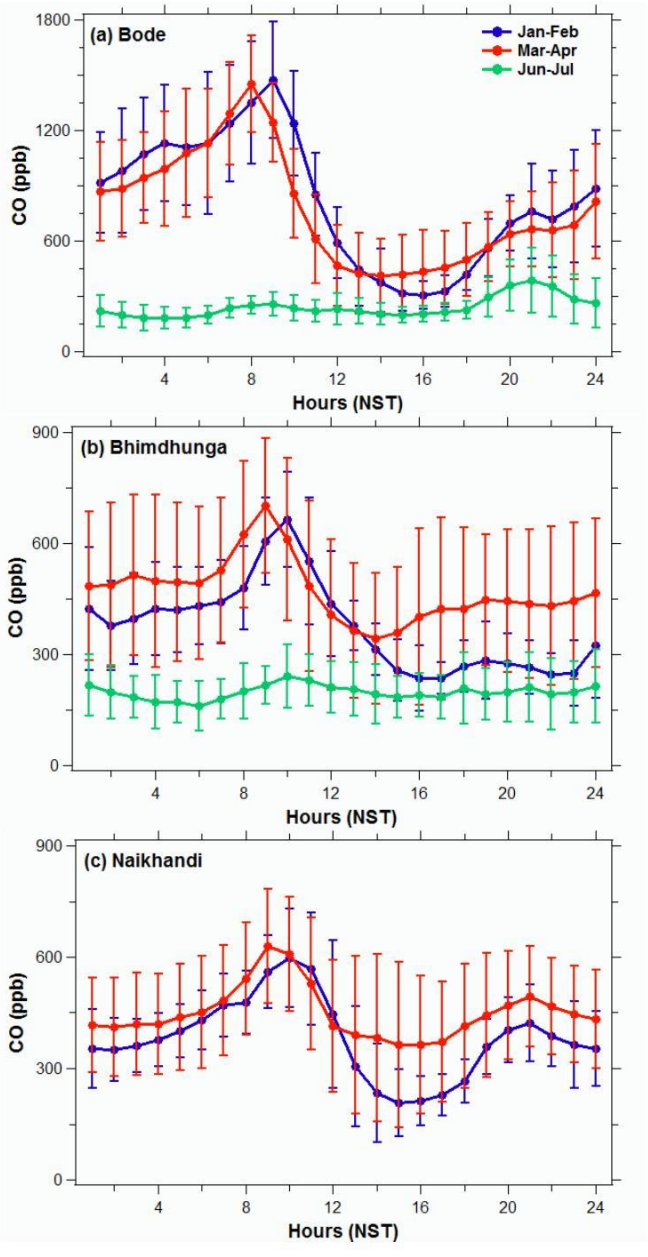

Figure 4. Comparison of diurnal variation of hourly average CO mixing ratios for four seasons at Bode,Bhimdhunga and Naikhandi. Due to the lack of continuous data at some sites, data of one month in each season were taken for comparison as representative of the winter (16 Jan – 15 Feb), pre-monsoon (16 Mar – 15 Apr) and monsoon (16 Jun – 15 Jul) season of 2013. Note: y-axis scale of the top figure (Bode) is double than lower panel two sites (Bhimdhunga and Naikhandi).

Atmos. Chem. Phys. Discuss., https://doi.org/10.5194/acp-2017-709
Manuscript under review for journal Atmos. Chem. Phys.
Discussion started: 18 December 2017

Atmospheric Chemistry and Physics Discussions

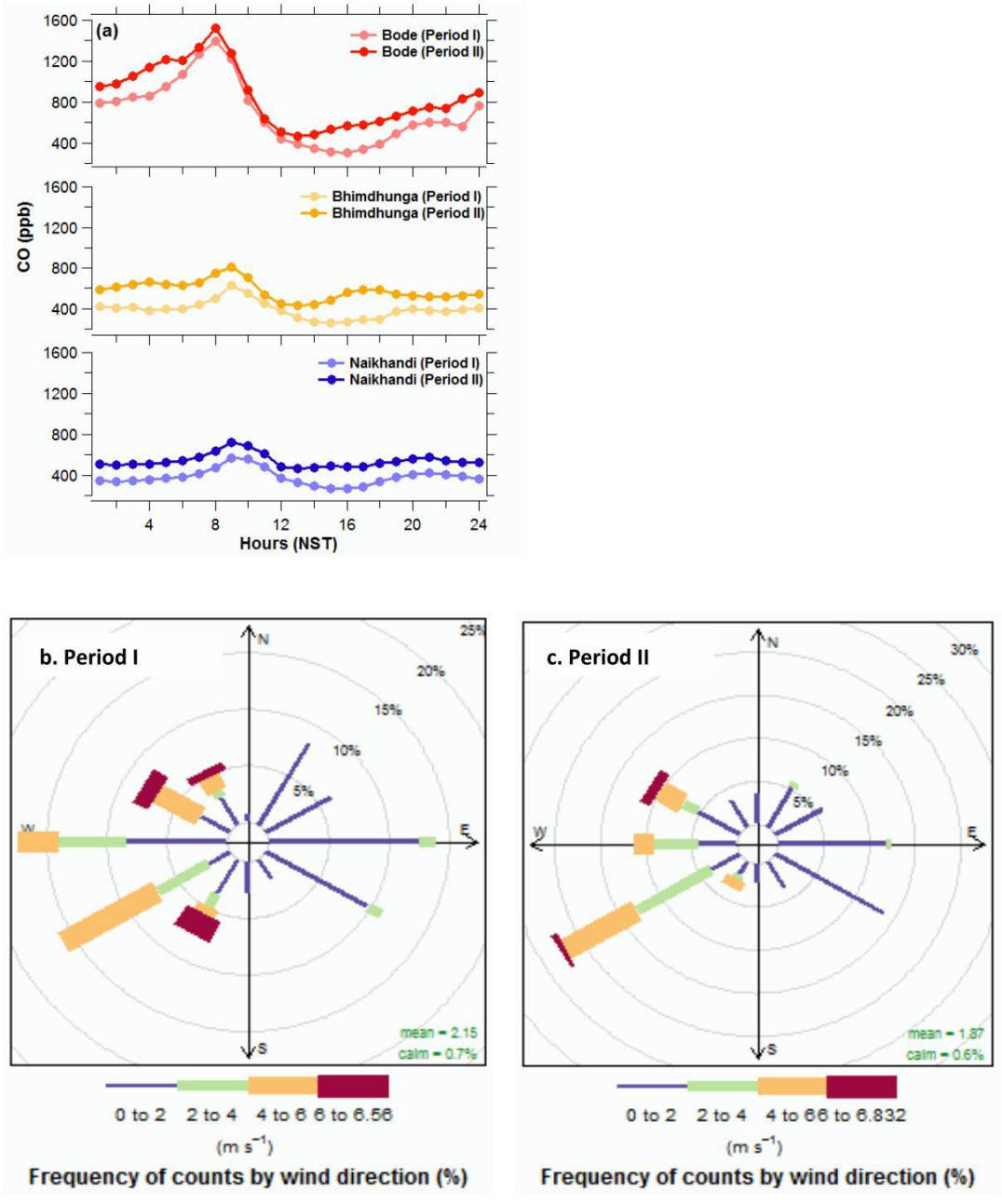

Figure 5. Comparison of hourly average CO mixing ratios during normal days (March 16-30), labelled as period I (faint color) and episode days (April 1-15), labelled as period II (dark color) in 2013 at (a) Bode, Bhimdhunga and Naikhandi in the Kathmandu Valley. The wind roses at Bode corresponding to two periods are also plotted (b) period I and (c) period II respectively.

Atmos. Chem. Phys. Discuss., https://doi.org/10.5194/acp-2017-709
Manuscript under review for journal Atmos. Chem. Phys.
Discussion started: 18 December 2017

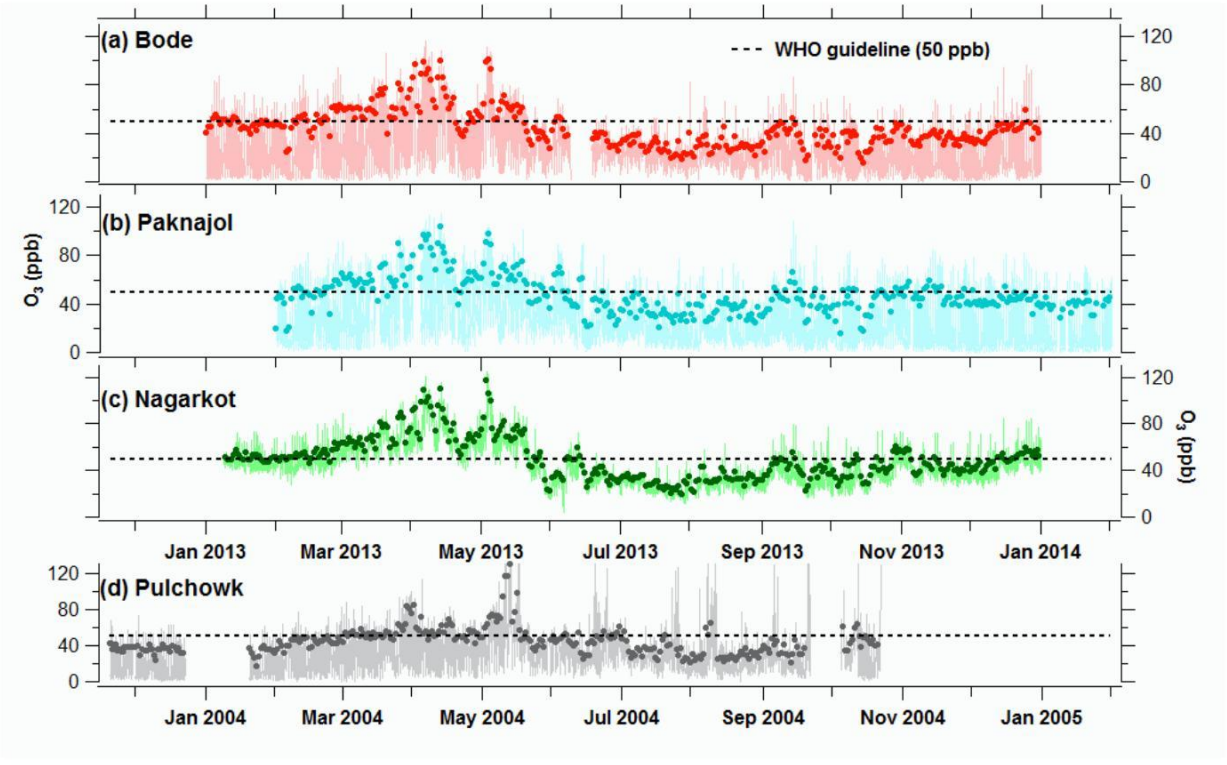

Figure 6. Time series of hourly average (faint colored line) and daily maximum 8-hr average (solid colored circle) O_3 mixing ratio at (a) Bode (semi-urban), (b) Paknajol (urban)and (c) Nagarkot (hilltop) observed during 2013-2014, and (d) Pulchowk (urban) observed during November 2003-October 2004 in the Kathmandu Valley. Black dotted line represents WHO guideline (50 ppb) for daily maximum 8-hour average of O_3.

Atmos. Chem. Phys. Discuss., https://doi.org/10.5194/acp-2017-709
Manuscript under review for journal Atmos. Chem. Phys.
Discussion started: 18 December 2017

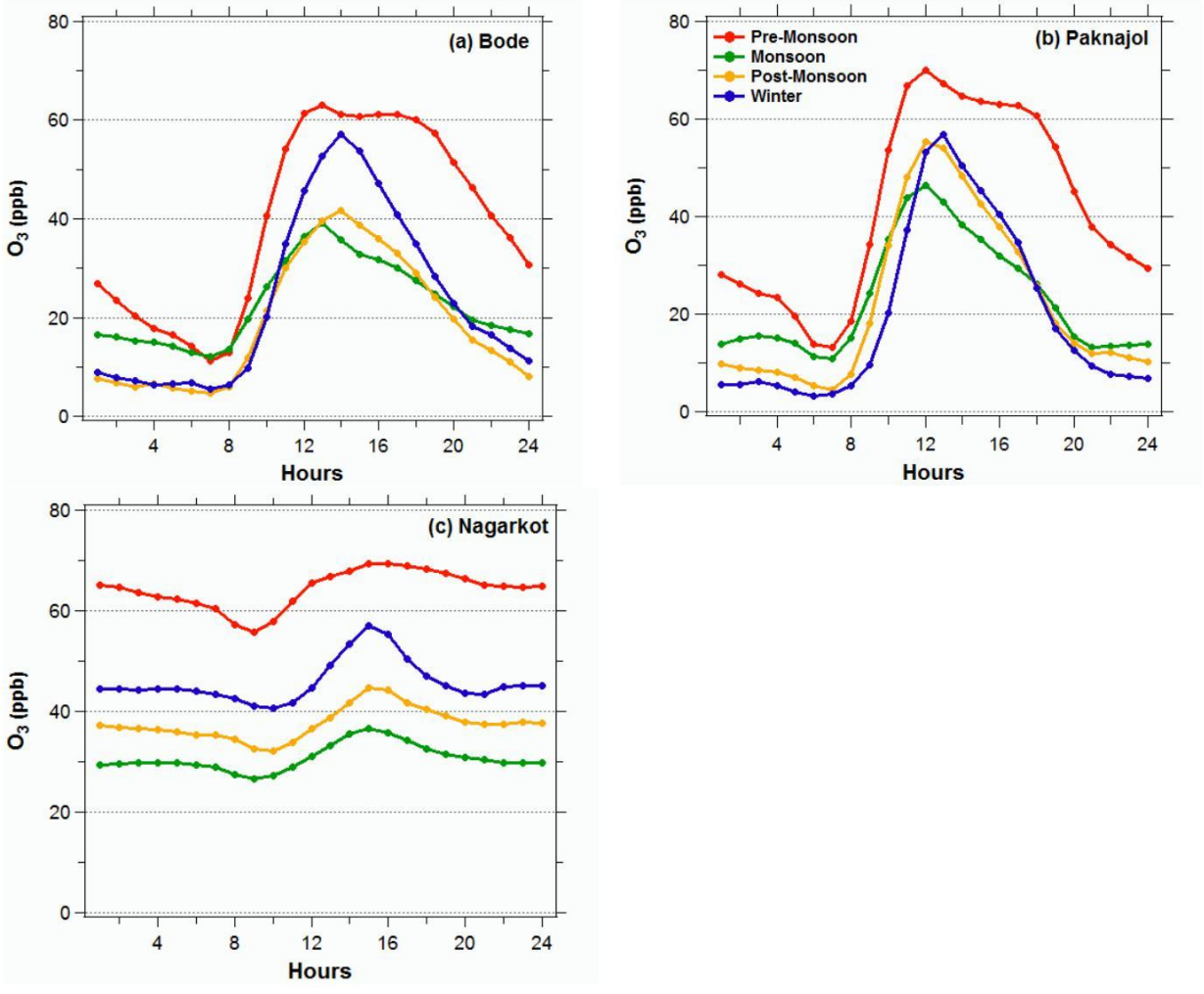

Figure 7. Diurnal pattern of hourly average O_3 mixing ratio for different seasons during January 2013-January 2014 at (a) Bode, (b) Paknajol, and (c) Nagarkot in the Kathmandu Valley. The four seasons (described in the text) are defined as: pre-monsoon (Mar-May), monsoon (Jun-Sep), post-monsoon (Oct-Nov), winter (Dec-Feb).

Atmos. Chem. Phys. Discuss., https://doi.org/10.5194/acp-2017-709
Manuscript under review for journal Atmos. Chem. Phys.
Discussion started: 18 December 2017

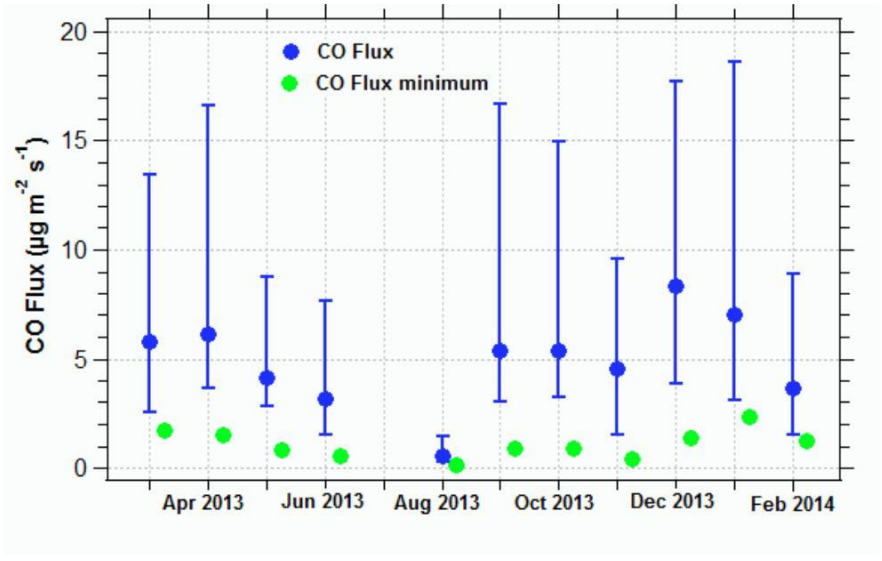

Figure 8. The estimated monthly average CO emission flux, which is based on the mean diurnal cycle of CO mixing ratios of each month for two conditions: (i) with data of all days (CO Flux) (blue dot) with lower and upper ends of the bar representing 25th and 75th percentile respectively, and (ii) with data of morning hours (CO Flux minimum (green dot) in which zero emission is assumed for the other hours of the day. The fluxes for July were not estimated as there were insufficient (less than 15 days) of concurrent CO and mixing layer height data. It is expected that the F_{CO} and $F_{COmin.}$ for July should fall between values for June and August 2013.